X-Ray imaging of inhomogeneous objects by coherent wave (phase contrast)

Victor Kohn

Russian Research Centre "Kurchatov Institute", 123182 Moscow, Russia

date: May, 1998; file: hl-phase.ps

The document is the part of Hamburg lectures
"Selected topics in the theory of coherent scattering of X-rays"

Contents:

1. Geometrical optics of inhomogeneous waves
2. Small angle approximation
3. What we see on the X-ray image of the object
4. X-Ray topography and Takagi equations
5. The propagators of two-beam diffraction
6. Review of first results of phase contrast imaging

    6.1 Refraction contrast in X-ray introscopy

    6.2 X-ray plane-wave topography observation of the phase contrast from a non-crystalline object

    6.3 Demonstration of phase-contrast X-ray computed tomography using an X-ray interferometer

    6.4 Quantitative Phase Imaging Using Hard X Rays

    6.5 Phase Contrast Microimaging by Coherent High Energy Synchrotron Radiation in experimental set-up of in-line holography

7. The theory of plane wave imaging
8. The theory of in-line imaging

    8.1 The propagator and the problem of coherence

    8.2 The conditions of image formation

9. The problem of the phase retrieval from intensity in in-line holographic scheme

    9.1 Standard object reconstruction algorithms for far-field conditions

    9.2 The problem of the phase retrieval under the near-field condition

1. GEOMETRICAL OPTICS OF INHOMOGENEOUS WAVES

To understand better the subsequent questions let us begin from the simplest approach of optics known as geometrical optics. Namely, let us consider the medium having the middle complex susceptibility $\chi(\mathbf{r}) = \chi'(\mathbf{r}) + i\chi''(\mathbf{r})$ slowly varying in space compared to the wavelength $\lambda = 2\pi c/\omega$ of spatially inhomogeneous monochromatic wave of frequency ω (c is a speed of light). We write the wave field as

$$E(\mathbf{r}) = I^{1/2}(\mathbf{r}) \exp\left[i\phi(\mathbf{r})\right], \qquad I(\mathbf{r}) = |E(\mathbf{r})|^2. \tag{1}$$

where $I(\mathbf{r})$ is a wave intensity. The Maxwell's equation may be written in the form

$$[-\mathrm{grad}^2 - K^2]E(\mathbf{r}) = K^2\chi(\mathbf{r})E(\mathbf{r}), \qquad K = \omega/c \tag{2}$$

where K is a wave number of monochromatic wave. The equation is valid at least in an approximation of electric dipole interaction between the wave and the matter.

Now let us take into account that the intensity cannot change quickly because in opposite case the wave either disappears or will be of great intensity which is out of the real life. As for the phase $\phi(\mathbf{r})$, it can change with arbitrary speed. Therefore we may neglect the second derivative of the intensity. Bearing this in mind we substitute the wave field of Eq.(1) in the Eq.(2). After the accurate calculating the first and second derivatives we obtain

$$iI^{-1/2}\mathrm{grad}\,\phi\mathrm{grad}\,I + i[K^2\chi'' + \mathrm{grad}^2\phi]I^{1/2} = ((\mathrm{grad}\,\phi)^2 - K^2(1+\chi'))I^{1/2} \tag{3}$$

Here the left-hand side has a pure imaginary value while the right-hand side has a pure real value. To satisfy the equation we need to put both sides to be equal zero. Therefore we have two equations

$$\mathbf{k}(\mathbf{r})\mathrm{grad}\,I(\mathbf{r}) = [K^2\chi''(\mathbf{r}) + \mathrm{grad}^2\phi]I(\mathbf{r}), \qquad \mathbf{k}(\mathbf{r}) = \mathrm{grad}\,\phi(\mathbf{r}), \tag{4}$$

$$(\mathrm{grad}\,\phi)^2 = K^2(1+\chi'), \qquad |\mathbf{k}(\mathbf{r})| = K(1+\chi'(\mathbf{r}))^{1/2} \tag{5}$$

Let us examine what we have obtained. The second equation is a pure equation for the phase $\phi(\mathbf{r})$. Moreover, it defines directly the modulus of the local wave vector of local ray. To calculate the phase distribution we need to start from the surface of constant phase. Then in each point $\mathbf{r}$ of this surface the direction of ray or local wave vector $\mathbf{k}(\mathbf{r}) = \mathrm{grad}\,\phi(\mathbf{r})$ is just perpendicular to the surface (see Fig.1(left)). Let s be a coordinate along this direction. Then the equation for the phase along the ray takes a simple form and can be easily solved

$$\frac{d\phi}{ds} = K(1+\chi'(s))^{1/2}, \qquad \phi(s) = \phi(s_0) + K\int_{s_0}^{s} ds_1(1+\chi'(s_1))^{1/2} \tag{6}$$

where s_0 is a coordinate on the ray which corresponds to initial surface. However, we cannot go along the ray so much because the direction of the ray is determined by initial surface. Therefore we may consider all rays on the initial surface and choose the distance

l on each ray as being less compared to characteristic length of susceptibility change on one hand, and leading to the definite value of phase change. Therefore the distance l is the distance of constant optical path. The new surface as a geometrical place of ends of all rays will be once again the surface of constant phase but its curvature may be changed. We define the new directions of ray and repeat the procedure and so on.

Thus, we may calculate the phase of wave field in all space. It is clear that this procedure cannot be accurate infinitely. It is the way of simple geometrical approximate solution of the Maxwell's differential equation. It is difficult to imagine or to represent the Maxwell's equation but it is easy to draw the rays. On the other hand, we now understand that the method is good only on small distances from the known surface of constant phase and only for a slow change of the electronic density inside the matter. If the medium is homogeneous, namely, the susceptibility χ is a constant, then the optical path is proportional to the real path of rays. One can verify directly that in this case the direction of rays stay the same independently of distance from the initial surface. It is remarkable property of geometrical optics that the rays may converge, intersect each other and diverge after that, giving the approximately right solution for the phase.

The next step is the calculation of the intensity along the rays. For this we have well defined the approximate equation

$$\mathbf{k}(\mathbf{r})\mathrm{grad}\, I(\mathbf{r}) = K^2\chi''(\mathbf{r})I(\mathbf{r}) \tag{7}$$

where we neglect the second derivatives of the phase considering these as small ones. It is new approximation of the method. This is consistent with the pointed above condition that the susceptibility is a slow function. However, near the focus of radiation the second derivative may be large independently on the property of the matter. Therefore the geometrical optics does not work in the region near the focus. In other regions we introduce once again the coordinate s along the ray and we have

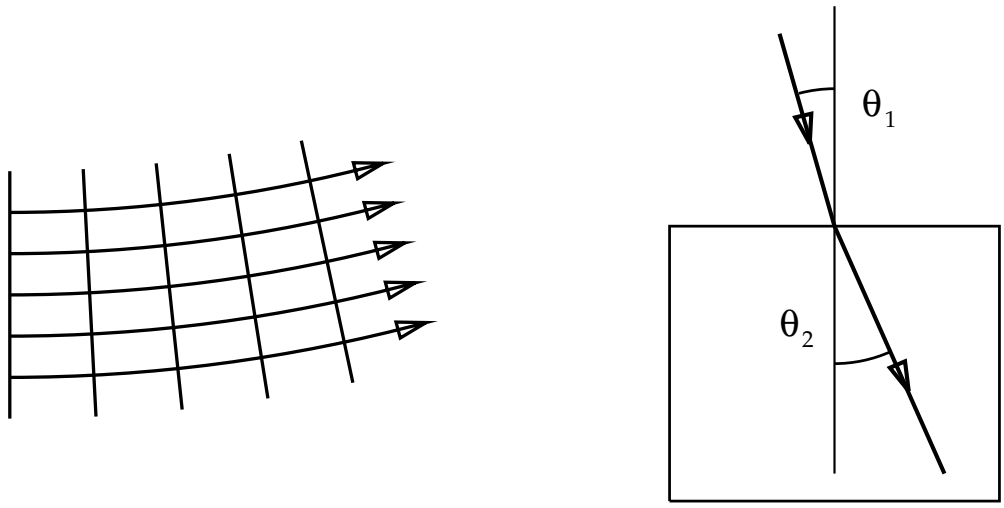

FIG. 1. The rays are perpendicular to the surface of constant phase (left) and satisty to the Fresnel law of refraction at the boundary between two homogeneous media (right)

$$\frac{dI(s)}{ds} = \frac{K^2}{|\mathbf{k}(s)|}\chi''(s)I(s), \qquad I(s) = I(s_0)\exp\left(\int_{s_0}^{s} ds_1 \frac{K^2}{|\mathbf{k}(s_1)|}\chi''(s_1)\right) \tag{8}$$

The very important property of geometrical optics is that each ray satisfies locally the Fresnel law of refraction of the ray at the boundary between two homogeneous media. This law is the same as the Fresnel formula for the plane wave in all cases excluding the glancing incidence, namely,

$$n_1 \sin\theta_1 = n_2 \sin\theta_2, \qquad n_i = (1+\chi_i)^{1/2}, \qquad i = 1,2 \tag{9}$$

Here θ_1 and θ_2 are the angles between the rays before and after the boundary and the normal to the boundary (Fig.1(right)) Even these two rules:
(1) the direction of ray is constant in homogeneous medium,
(2) the rays change the direction at the boundary of two homogeneous media according to the Fresnel formula of refraction,
allow to calculate the properties of many optical systems like set of many lenses of different shape.

2. SMALL ANGLE APPROXIMATION

In the small angle approximation one assumes that the wave field differs only slightly from the plane wave with the wave vector $\mathbf{k}_0$ having the modulus $|\mathbf{k}_0| = K$. So the total phase $\phi(\mathbf{r})$ can be written now as

$$\phi(\mathbf{r}) = \mathbf{k}_0\mathbf{r} + \varphi(\mathbf{r}), \qquad \mathrm{grad}\,\phi = \mathbf{k}_0 + \mathrm{grad}\,\varphi \tag{10}$$

where $\mathrm{grad}\,\varphi$ is much less compared to $\mathbf{k}_0$. It is possible only if $\chi(\mathbf{r}) \ll 1$, the situation which just takes place in case of hard X-ray scattering. Let us use this inequality in explicit form. It is necessary because it is difficult to calculate the small values simultaneously with large values. At least we shall have errors using the computer which makes the calculations with limited accuracy. The general equation for the phase

$$(\mathrm{grad}\,\phi)^2 = K^2(1+\chi') \tag{11}$$

takes the approximate form like this

$$|\mathbf{k}_0|^2 + 2\mathbf{k}_0\mathrm{grad}\,\varphi(\mathbf{r}) = K^2(1+\chi'), \qquad 2\mathbf{k}_0\mathrm{grad}\,\varphi(\mathbf{r}) = K^2\chi'(\mathbf{r}) \tag{12}$$

The last equation shows that we can neglect the small deviation of rays from the base direction $\mathbf{k}_0$ and calculate the phase change introducing the coordinate along the $\mathbf{k}_0$.

Let now this coordinate be z. Then we have

$$\frac{d\varphi(\mathbf{r})}{dz} = \frac{1}{2}K\chi'(\mathbf{r}). \tag{13}$$

Similar equations we obtain for intensity and for amplitude of the wave

$$\frac{dI(\mathbf{r})}{dz} = K\chi''(\mathbf{r})I(\mathbf{r}), \qquad \frac{dI^{1/2}(\mathbf{r})}{dz} = \frac{1}{2}K\chi''(\mathbf{r})I^{1/2}(\mathbf{r}) \tag{14}$$

These equations shows that the small angle approximation allows to simplify the problem. We may keep the direction of rays the same for all points in the transverse plane normal to the base wave vector and we need to calculate only the phase change and the wave amplitude change along this direction. We may write the both equations as one equation for the complex value

$$E_0(\mathbf{r}) = I^{1/2}(\mathbf{r}) \exp\left(i\varphi(\mathbf{r})\right), \qquad E(\mathbf{r}) = E_0(\mathbf{r}) \exp(i\mathbf{k}_0\mathbf{r}) \tag{15}$$

as

$$\mathbf{k}_0 \mathrm{grad}\, E_0(\mathbf{r}) = \frac{i}{2} K^2 \chi(\mathbf{r}) E_0(\mathbf{r}) \tag{16}$$

Such an equation may be called as Takagi equation in one beam approximation using the language of the modern X-ray diffraction optics (or X-Ray crystal optics). The physical sense of this approximation is very clear. We have the wave which quickly oscillates in space with the constant wavelength λ but the amplitude of this wave and the additional aperiodic phase shift are the slow functions of space with characteristic length of change much larger then the base wavelength λ. This is quite similar to the technique of radio-physics were the sound wave used to modify the amplitude of radio wave having much shorter wavelength. Such an extra wave is called an envelope wave. However, similar situations arise in many physical phenomena when some fast process goes together with some slow process. The method of considering is always the same. The variables are divided on fast variables and slow variables. If we are interested in the fast process then we can regard the slow process as being unchanged completely and consider the slow variables as constant. If we are interested in slow process then we need to exclude the fast variable from the equations. So the Eq.(16) is just the Maxwell's equation after the excluding the fast variable.

3. WHAT WE SEE ON THE X-RAY IMAGE OF THE OBJECT

Let us introduce the Cartesian coordinate system x, y, z with z-axis along the optical axis. The Eq.(16) can be rewritten as

$$\frac{dE_0(x,y,z)}{dz} = \frac{i}{2} K \chi(x,y,z) E_0(x,y,z). \tag{17}$$

Let us choose the plane (x, y) at $z = z_0$ just before the object having unknown structure. If all devices before the object are known we may calculate the wave field from the source through all devices. Therefore we know the function $E_0(x, y, z_0)$. This may be the plane wave when $E_0(x, y, z_0)$ does not depend on x, y or the spherical wave in the small angle approximation when

$$E_0(x,y,z_0) = \frac{1}{z_0} \exp\left(iK\frac{x^2+y^2}{2z_0}\right). \tag{18}$$

The plane wave may be treated as a particular case of spherical wave at very large distance z_0.

Let us choose another plane at $z = z_1$ just after the object. The wave field at this plane is obtained from the solution of Eq.(17) as follows

$$E_0(x, y, z_1) = E_0(x, y, z_0) \exp\left(\frac{i}{2} K \int_{z_0}^{z_1} dz'\, \chi'(x, y, z')\right) \exp\left(-\frac{K}{2} \int_{z_0}^{z_1} dz'\, \chi''(x, y, z')\right). \tag{19}$$

This expression shows that both the amplitude and the phase of the X-ray wave is changed by the object. The phase change is proportional to integral over path of X-ray beam decrement of refractive index $\delta = \chi'/2$, namely

$$\Phi(x, y) = \frac{2\pi}{\lambda} \int_{z_0}^{z_1} dz'\, \delta(x, y, z') \tag{20}$$

while the amplitude change is determined by the total absorption of X-ray beam along the optical axis and allows to obtain the integral index of absorption.$\beta = \chi''/2$, namely

$$M(x, y) = \frac{2\pi}{\lambda} \int_{z_0}^{z_1} dz'\, \beta(x, y, z') \tag{21}$$

Both functions depend on the internal structure of the object through the integral. And both functions give the projection of the object along the optical axis as an image like the photographic image.

What we shall see really depends on the kind of source and kind of detector. If we use quasi-point source (the source having the size less than the details of the object) and we use a film just after and close to the object as a position sensitive detector then each point of the film feels only the intensity of the ray incoming to this point. Therefore we may obtain only the slightly magnified map of the integral index of absorption. Such a technique is widely used today in different spheres of our life, including the diagnostic of human body in medicine. However, this technique demands the X-ray to be absorbed inside the object. It is not easy, especially for small objects consisting of light atoms. For example, biological objects of 1 mm size and of middle density $\rho = 1$ g/cm^3 give the value of M-function about 1 to 2 percent for wavelength of radiation λ from 0.5 to 1 Å. For higher energy of X-rays the absorption drops rapidly therefore the imaging of microobjects (microimaging) is not possible in such a technique.

On the other hand, in medicine for diagnostic of human body it is undesirable that X-rays are absorbed in the body. In addition, the absorption technique may show only the parts of body containing a hard atoms having many electrons, mainly, the bones while the parts with a small difference of density cannot be distiguished. Summarizing all reasons presented above one can see that it is quite desirable to make visible the phase shift produced by the object. The specific feature of X-rays of high energy is that the decrement of refractive index δ is much larger than the index of absorption β. It is shown on Fig.2(left) that for X-Ray energy of 50 keV in Silicon $\delta \approx 1000\beta$ and in Boron $\delta \approx 100000\beta$. Therefore when the absorption contrast will show nothing completely the phase contrast can show something even for small object.

The value of δ is easy to estimate. In case of Rayleigh scattering giving the main contribution and monatomic medium we have

$$\delta = -\frac{\lambda^2 r_0}{2\pi} N Z = -\lambda^2 \rho C \frac{Z}{A}, \qquad C = 0.27 \cdot 10^{-5}. \tag{22}$$

where $r_0 = e^2/mc^2$ is the classical electron radius, λ is a wavelength in Å, N is a number of atoms in unit volume, Z is a number of electrons in the atom, A is a mass of atom in atomic units, ρ is a density in g/cm^3. For example, for the object containing Carbon atoms of thickness $t = 0.01\,\text{mm} = 10\,\mu\text{m}$ and for energy of X-Rays 50 keV ($\lambda = 0.25\,$Å) we calculate ($\rho = 2.62\,\text{g/cm}^3$) that the phase shift equals $\Phi = 0.5$ that can be apparently registered. On the other hand, the absorption contrast will be hundred times less than per cent.

In principle, it is not difficult to see the phase shift even using the film. For this we need to place the film far from the object. Because the object produces an inhomogeneous phase shift the rays change their directions in the following passage through the empty space (see Fig.2(right)).

At some large enough distance after the object the density of rays becomes inhomogeneous that leads to the inhomogeneous intensity which can be registered. The problem is only that the angle of deviation is very small therefore for small distances the size of such an image will be also small especially for small object. Therefore the requirement on the coherence of the radiation, namely, on the transverse source size, is rather high. Nevertheless, this simple scheme of in-line holography with small a size of projection of the source and large a distance from the source to detector compared to the size of object is successfully realized today on the synchrotron radiation sources of third generation (for example, ESRF, France). However, simultaneously with this technique, a rather different technique is used now which can work with the usual sources of radiation and does not demand large distances in the experimental setup. Instead of this the perfect crystal -

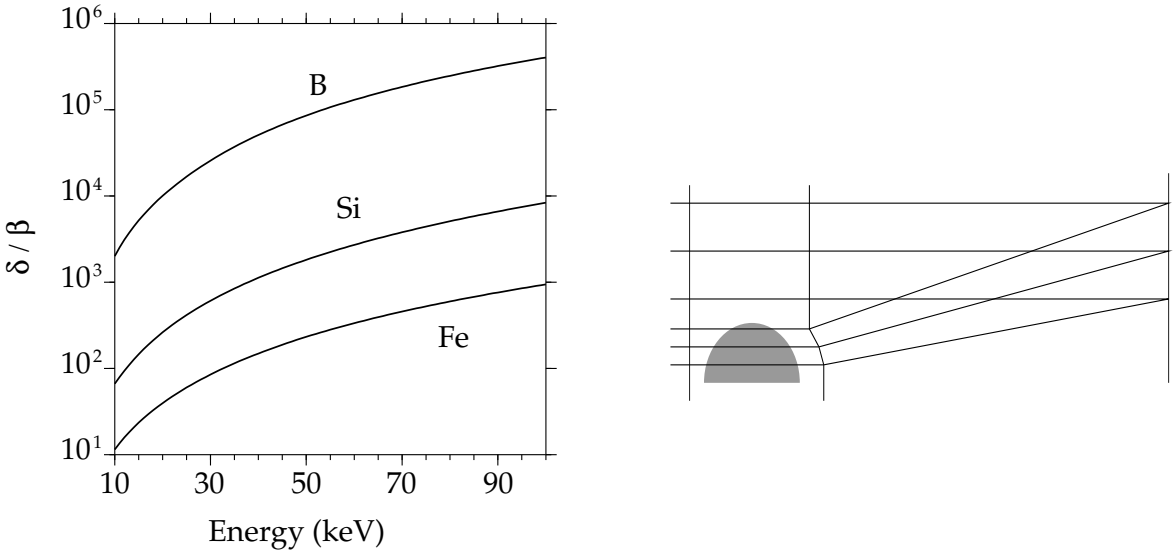

FIG. 2. The relation of decrement of refractive index δ to index of absorption β is a growing function of energy of X-rays (left), the object always incline the X-ray out of its shadow (right)

collimator - is used for preparing the incident quasi-plane wave and second perfect crystal - analyzer - is used for a registration of local angular deviations of the rays. This technique goes from the well developed preceding technique of imaging of crystal lattice defects in single crystals called X-Ray topography.

The first step in the theoretical foundation of the technique of X-ray topography was made by Takagi who writes the equations describing the interference of X-ray beams inside the slightly deformed crystal lattice. Let us shortly consider the principles of X-ray topography which allows to understand better the technique which uses the perfect crystals.

4. X-RAY TOPOGRAPHY AND TAKAGI EQUATIONS

We know that the crystal lattice is a periodical structure, therefore the susceptibility of the crystal satisfy the translational symmetry and can be expanded as a Fourier sum over the reciprocal lattice vectors

$$\chi_{id}(\mathbf{r}) = \sum_{\mathbf{h}} \chi_{\mathbf{h}}^{(id)} \exp(i\mathbf{hr}), \qquad \chi_{\mathbf{h}}^{(id)} = \frac{1}{V_0} \int d\mathbf{r}\, \chi_{id}(\mathbf{r}) \exp(-i\mathbf{hr}) \tag{23}$$

Here V_0 is a volume of the unit cell and the integration is carried out over this volume. What happens when atoms are displaced from its positions in perfect crystal lattice. We may neglect the change of inner structure of electronic density of the atoms near the defect of crystal lattice. Therefore we shall suppose that atoms are displaced as a whole. Then we have a relation

$$\chi(\mathbf{r} - \mathbf{u}(\mathbf{r})) = \chi_{id}(\mathbf{r}) = \sum_{\mathbf{h}} \chi_{\mathbf{h}}^{(id)} \exp(i\mathbf{hr}) \tag{24}$$

where $\mathbf{u}(\mathbf{r})$ is just a displacement of the atoms near the defect which depends on the local position of the atom.

The crystal lattice in large volume has the same reciprocal lattice vectors therefore we need now to calculated the Fourier coefficients of real susceptibility over the ideal reciprocal lattice vectors. So we multiply the $\chi(\mathbf{r})$ by $\exp(-i\mathbf{hr})$ and integrate over the unit cell

$$\chi_{\mathbf{h}}(\mathbf{r}) = \frac{1}{V_0} \int d\mathbf{r}\, \chi(\mathbf{r}) \exp(-i\mathbf{hr}) \tag{25}$$

Now let us use the Eq.(24) which gives us the formula

$$\chi_{\mathbf{h}}(\mathbf{r}) = \frac{1}{V_0} \int d\mathbf{r}\, \chi_{id}(\mathbf{r} + \mathbf{u}(\mathbf{r})) \exp(-i\mathbf{hr}) = \frac{1}{V_0} \int d\mathbf{r}\, \chi_{id}(\mathbf{r}) \exp(-i\mathbf{hr} + \mathbf{ihu}(\mathbf{r}))$$

where in the last integral we shifted the region of integration to the position of unit cell in the ideal crystal. In the following we shall restrict ourselves by only the cases where the displacement of atoms is a slow function of the coordinate and it may be considered as a constant inside the unit cell. This takes place, for example, in the region far from the core of dislocation but this is not such in the core of dislocation. However, such regions

where this condition does not meet, is usually very small. Considering $\exp(\mathbf{ihu}(\mathbf{r}))$ as a constant inside the unit cell we immediately obtain the relation

$$\chi_{\mathbf{h}}(\mathbf{r}) = \chi_{\mathbf{h}}^{(id)} \exp(\mathbf{ihu}(\mathbf{r})) \tag{26}$$

This relation shows that the susceptibility of disturbed crystal lattice does not influence the incident beam but it leads to an additional phase shift in the diffracted beam so we obtain the inhomogeneous medium. For solving the task we shall use once again the geometrical optics approach in the small angle approximation. In the two-beam case of diffraction we try the solution in the form

$$E(\mathbf{r}) = E_0(\mathbf{r}) \exp(i\mathbf{k}_0\mathbf{r}) + E_h(\mathbf{r}) \exp(i\mathbf{k}_h\mathbf{r}) \tag{27}$$

where $\mathbf{k}_h = \mathbf{k}_0 + \mathbf{h}$ and the complex amplitudes $E_0(\mathbf{r})$ and $E_h(\mathbf{r})$ are the slow functions of the coordinates compared to exponent functions.

Substituting this form of solution to the Maxwell's equation and integrating over the unit cell, as before, we obtain the set of equations for the slow functions only

$$\begin{aligned} \mathbf{k}_0 \mathrm{grad} E_0 &= \frac{i}{2} K^2 \left[\chi_0 E_0 + \chi_{\overline{h}} \exp(-i\mathbf{hu}(\mathbf{r})) E_h\right] \\ \mathbf{k}_h \mathrm{grad} E_h &= \frac{i}{2} K^2 \left[\chi_h \exp(i\mathbf{hu}(\mathbf{r})) E_0 + (\chi_0 - \alpha) E_h\right] \end{aligned} \tag{28}$$

where $\alpha = (\mathbf{k}_h^2 - K^2)/K^2$ is a usual parameter of deviation from the Bragg condition and the Fourier components of susceptibility relate to the ideal crystal lattice where the index (id) is omitted for the sake of writing convenience, $\chi_{\overline{h}}$ is the Fourier component for the reciprocal lattice vector $-\mathbf{h}$. The equation (28) was proposed for the first time by Takagi in a short article

- S. Takagi, Acta Crystallogr., 1962, vol. 15, p. 311

and is called now Takagi equations. Later the equations of such a type was used by Taupin for calculating first topographic images of dislocations in the article

- D. Taupin, Bull. Soc. Fr. Mineral. Crystallogr., 1964, vol. 87, p. 469.

therefore sometimes the equations are called Takagi-Taupin equations.

The Eqs.(28) are really very useful and powerful technique for calculating the images of different crystal lattice defects. These have a clear physical meaning. In the two-beam case of diffraction we must consider the two sets of rays - along the incident beam and along the diffracted beam. However, considering the trajectory along for the incident beam, for example, we need to take into account a possibility of local crystal lattice to scatter the wave from the diffracted ray to the incident ray. Therefore the wave along the incident ray feels the influence of waves along the diffracted ray which intersect the considering point. The same takes place for the rays along the diffracted wave. In numerical computer calculating the images this picture is implemented really in the computer program. In the ideal crystal the processes of scattering from the incident ray to the diffracted ray and vice versa beam are the same for all points of the crystal volume. In the distorted crystal lattice the processes of scattering is accompanied by the local phase shift in the waves which leads to the inhomogeneous intensity of the waves at the exit surface of the crystal.

The geometrical picture of scattering allows to draw the possible region of the crystal which contribute to given point on the exit surface. In the Laue case of diffraction this region is always finite (see Fig.3(left)) while in the Bragg case the region is infinite but the main contribution goes from the area close to given point (see Fig.3(right)). The integral form of the Takagi equations was derived in the paper

- A. M. Afanasev, V. G. Kohn, Acta Crystallogr. 1971, vol. A27, p. 421.

The integral form of equations is a partial solution of the equations because integral equations allow us to represent the wave field at the point of interest as a contribution of wave fields over the possible region. These solve also the problem of boundary conditions in the case when the incident wave is inhomogeneous. Just this problem is of interest for us - what happens when the inhomogeneous wave falls on the perfect crystal.

5. THE PROPAGATORS OF TWO-BEAM DIFFRACTION

The Laue case is more simple one therefore it may be represented here in detail. Let us consider the crystal in the form of the plane parallel plate of thickness t. Let us introduce the coordinates z along the normal to the surface and x along the surface in the plane of scattering which is determined by the vectors $\mathbf{k}_0$ and $\mathbf{k}_h$. The entrance surface corresponds to $z = 0$ while the exit surface corresponds to $z = d$. The incident wave has the amplitude $E_0(x, 0) = A(x)$ at the entrance surface while the diffracted surface $E_h(x, 0) = 0$. The task consists of finding the equations for the wave field $E_0(x, d)$ and $E_h(x, d)$ at the exit surface. There are many ways to make a solution of the task. We may use the results of another topic of these lectures where the theory of X-ray plane wave diffraction is presented. For this purpose let us use the linear property of the equations and represent the known wave field $A(x)$ as a Fourier integral over the plane waves

$$A(x) = \int \frac{dq}{2\pi} A(q) \exp(iqx), \qquad A(q) = \int dx A(x) \exp(-iqx) \tag{29}$$

We may try the solution now in the form

$$E_0(x, d) = \int \frac{dq}{2\pi} A(q)\, t(q, d) \exp(iqx), \quad E_h(x, d) = \int \frac{dq}{2\pi} A(q)\, r(q, d) \exp(iqx) \tag{30}$$

where the functions $t(q, d)$ and $r(q, d)$ are the transmission and reflection amplitudes for the plane wave with the wave vector $\mathbf{k}_0 + q\mathbf{e}_x$ where $\mathbf{e}_x$ is a unit vector along the x-axis. The solution can be obtained from the known solution for the plane wave with the wave vector $\mathbf{k}_0$ through a simple replacement χ_0 by $\chi_0 - 2k_{0x}q/K^2$ and α by $\alpha_q = \alpha + 2h_x q/K^2$. We restrict ourselves by the case of symmetrical geometry when $k_{0z} = k_{hz}$ and the crystals having an inversion centre when $\chi_h = \chi_{\overline{h}}$. Using the results of pointed above topic we write the expressions for these amplitudes as follows

$$\begin{aligned} t(q, d) &= F_0 F_\alpha(-x_d) \left(\cos(s_q B x_d) + i \frac{\alpha_q}{2\chi_h s_q} \sin(s_q B x_d) \right), \\ r(q, d) &= i F_0 F_\alpha(-x_d) \frac{\sin(s_q B x_d)}{s_q} \end{aligned} \tag{31}$$

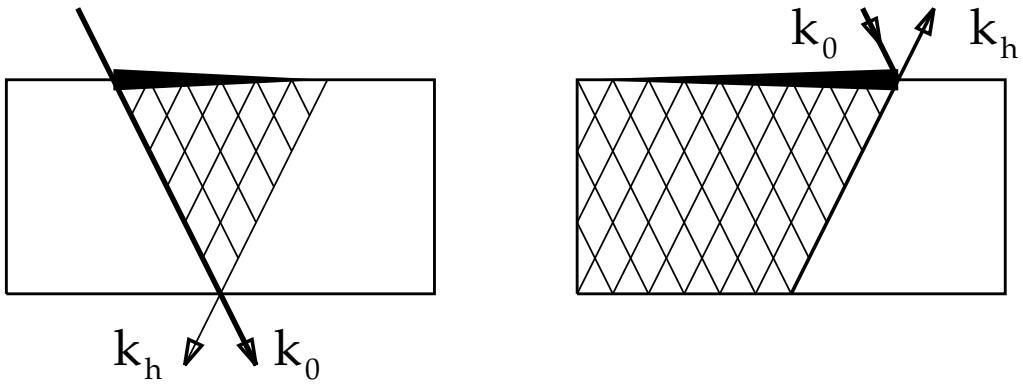

FIG. 3. The region of scattering (Borrmann delta) in the Laue case (left) and in the Bragg case (right) of X-ray diffraction

where

$$F_0 = \exp(\frac{i\pi\chi_0}{\lambda\cos\theta_B}d), \quad F_\alpha(x) = \exp(iCx), \quad C = \frac{\pi\alpha}{2\lambda\sin\theta_B},$$
$$s_q = \sqrt{1+(\alpha_q/2\chi_h)^2}, \quad \alpha_q = \alpha - \frac{4\sin\theta_B}{K}q, \quad B = \frac{\pi\chi_h}{\lambda\sin\theta_B}, \quad x_d = d\tan\theta_B. \qquad (32)$$

Now the problem is reduced to the calculation of the integrals of Eq.(30). However, it is not possible because we don't know the explicit expression for the function $A(q)$. Therefore instead of total solution we may use the property of Fourier integral and represents the Fourier component of the product of two functions as a convolution of the Fourier components of these functions.

$$E_0(x,d) = \int dx' P_{00}(x-x',d)A(x'), \quad E_h(x,d) = \int dx' P_{h0}(x-x',d)A(x') \qquad (33)$$

where the functions $P_{00}(x,t)$ and $P_{h0}(x,t)$ are the two-beam diffraction propagators of the field through the crystal which is defined as

$$P_{00}(x,d) = \int \frac{dq}{2\pi}\, t(q,d)\exp(iqx), \quad P_{h0}(x,d) = \int \frac{dq}{2\pi}\, r(q,d)\exp(iqx) \qquad (34)$$

This way of calculation shows clearly that the crystal propagators are in fact the Fourier transformation of the plane wave propagator over the transverse component of wave vector. To obtain the analytical form of the propagator we need to calculated the integrals. It is really possible and the results were presented for the first time in the papers

- A. Authier, D. Simon, Acta Crystallogr., 1968, vol. A24, p. 517.,
- I. Sh. Slobodetskii, F. N. Chuchovskii, V. L. Indenbom,

. Pis'ma v Zhurn. Exp. i Teor. Fiz., 1968, vol. 8, p. 90 (in Russian).

In out notation the results look as follows

$$P_{00}(x,d) = F_0\left[\delta(x-x_d) - \frac{1}{2}BF_\alpha(x-x_d)\sqrt{\frac{x_d+x}{x_d-x}}\mathrm{J}_1\left(B\sqrt{x_d^2-x^2}\right)\right],$$
$$P_{h0}(x,d) = \frac{i}{2}BF_0F_\alpha(x-x_d)\mathrm{J}_0\left(B\sqrt{x_d^2-x^2}\right). \qquad (35)$$

Here $\mathrm{J}_0(x)$ and $\mathrm{J}_1(x)$ are the Bessel functions, $\delta(x-x_d)$ is the Dirac delta-function and the propagator equals zero outside the region $x^2 < x_d^2$.

In the Bragg case the situation is more complicated because the exit surface for reflected beam coincides with the entrance surface for the incident beam. Nevertheless, the problem was solved analytically in general case of asymmetrical diffraction and thin crystal including multiple reflection from bottom side in the paper

- A. M. Afanasev, V. G. Kohn, Acta Crystallogr. 1971, vol. A27, p. 421.

Here we consider only symmetrical diffraction and $\chi_h = \chi_{\overline{h}}$. In the case of thick crystal the problem may be solved by Fourier transformation once again.

$$E_h(x) = \int \frac{dq}{2\pi}A(q)\,r(q)\exp(iqx) = \int dx' P_{h0}(x-x')A(x') \qquad (36)$$

where

$$r(q) = i\frac{\chi_h}{y+\sqrt{y^2-\chi_h^2}}, \quad y = \chi_0 - \frac{\alpha}{2} - \frac{\lambda\cos\theta_B}{\pi}q \qquad (37)$$

Here the branch of square root having the positive imaginary part is expected. The propagator equals

$$P_{h0}(x) = \int \frac{dq}{2\pi}\,r(q)\exp(iqx) = i\exp(iCx)\frac{\mathrm{J}_1(Bx)}{x}\theta(x), \qquad (38)$$

where

$$C = \frac{\pi(\alpha-2\chi_0)}{2\lambda\cos\theta_B}, \qquad B = \frac{\pi\chi_h}{\lambda\cos\theta_B} \qquad (39)$$

and $\mathrm{J}_1(x)$ is a Bessel function once again, $\theta(x)$ is Heaviside step function which equals unity if $x > 0$ and zero otherwise.

The results we obtain show that if the inhomogeneous wave falls on the perfect crystal then the inhomogeneous wave will reflected or transmitted by the crystal. The correlation between the characters of inhomogeneity is determined by the propagator function and it is not so obvious. However, let us examine first what appears in the experiments.

6. REVIEW OF FIRST RESULTS OF PHASE CONTRAST IMAGING

The first experiment on X-Ray imaging was performed by Röntgen who discovered X-rays just obtaining the X-ray image of his wife hand. It was an absorption map image. The first phase shift image of non-crystalline object was obtained, probably, by Bonse and Hart in the middle of sixtieth in experiments with X-ray LLL interferometer. The direction of study with a collimator and an analyzer was opened by

- E. Forster, K. Goetz and P. Zaumseil, Krist. Tech., 1980, vol. 15, p. 937.

However, the systematic study of the possibilities of phase shift imaging is carried out only in recent time. Below several groups are presented.

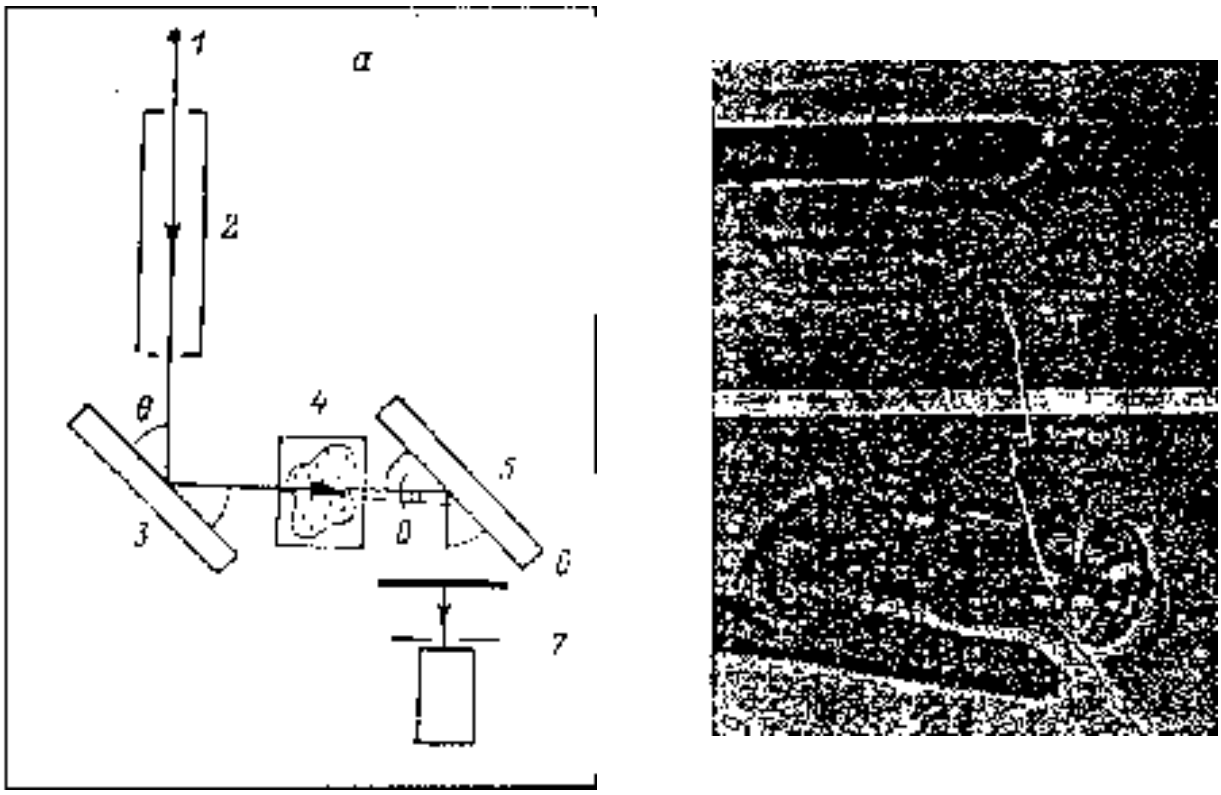

FIG. 4. The first experimental setup of Somenkov and Shilshtein group (left) and the first result of the fly imaging (right)

6.1 Refraction contrast in X-ray introscopy

One of the first group of new attack on the problem was V. A. Somenkov and S. Sh. Shilshtein group from "Kurchatov Institute" (Moscow, Russia). Other members of this group are A. K. Tkalich, A. A. Manushkin, N. L. Mitrofanov, K. M. Podurets. The first results were published in

- Zhurn. Tech. Fiz. 1991, vol. 61, p. 197 (Sov.Phys.-Tech.Phys, 1991, 36, 1309).

The approach is based on the angular analysis of radiation scattered by transparent (biological) object. Bragg case of diffraction is used for preparing the incident plane wave as well as for an angular analysis of transmitted radiation. When an absorption is significant in the object, the contrast becomes mixed, a refraction-absorption contrast.

In a first work the simplest experimental set-up was used with Si (333) symmetrical reflection and a scan by slit across the object when recording the image on the film (see Fig.4(left)). Fig.4(right) shows the comparison of pure absorption image of the fly (without a second Bragg analyzer, top image) and refraction image (bottom image). Despite of the poor quality of presented pictures (the originals were better) the higher sensitivity of the refraction contrast is seen. Today the author have improved the experimental implementation of the method (see. Fig.5). The improvement consists of:

(1) asymmetrical reflection for preparing the incident plane wave,

(2) two symmetrical Bragg reflections of higher order (511) for an analysis of inclined

rays owing to a refraction without the change of direction of the beam,

(3) a use of most sensitive part of the reflection curve at the boundary of the total reflection region.

The authors see the reason of the contrast in the fact that the rays with different directions are reflected by analyzing system with different powers. Therefore the sensitivity of the method depends on the degree of slope of the reflection curve. To obtain the better contrast the analyzer should be installed at the edge of the reflectivity maximum. Today the group is working on the first beamline of Kurchatov Institute synchrotron radiation source. They are going to develop the centre of medical diagnostic of biological objects including a human body.

6.2 X-ray plane-wave topography observation of the phase contrast from a non-crystalline object

Another group is working in X-ray laboratory of St. Petersburg in Russia. The authors are V. N. Ingal and E. A. Beliaevskaya, the first results is published in

- J. Phys. D: Appl. Phys. 1995, vol. 28, p. 2314.

They use practically the same technique of imaging of noncrystalline objects by means of local angular analysis of the transmitted beam. However, they use the Laue case of diffraction in the crystal-analyzer. This allows them to register simultaneously two images in transmitted beam and in reflected beam. An incident coherent beam is prepared by two crystals monochromators in an asymmetrical Bragg diffraction. The experimental

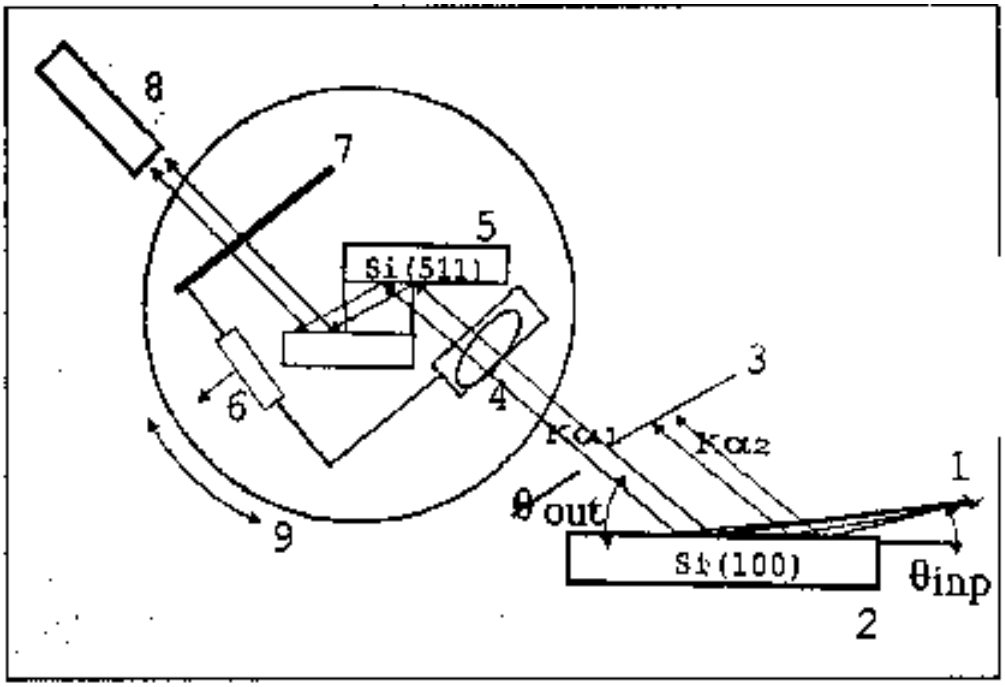

FIG. 5. The improved experimental setup of Somenkov and Shilshtein group

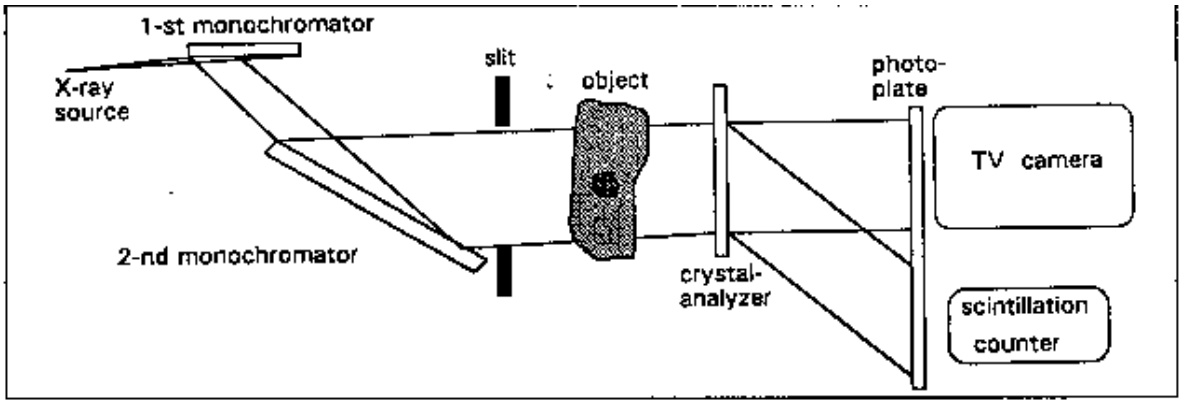

FIG. 6. The experimental setup of Ingal and Beliaevskaya

arrangement is shown in Fig.6.

The topographic images in the transmitted and reflected beams of the analyzer were called Phase Dispersion Images (PDI). The X-ray tubes with Mo K_α and Ag K_α anodes were used, the exposure time was about 20 min. The 220 asymmetrical diffraction was

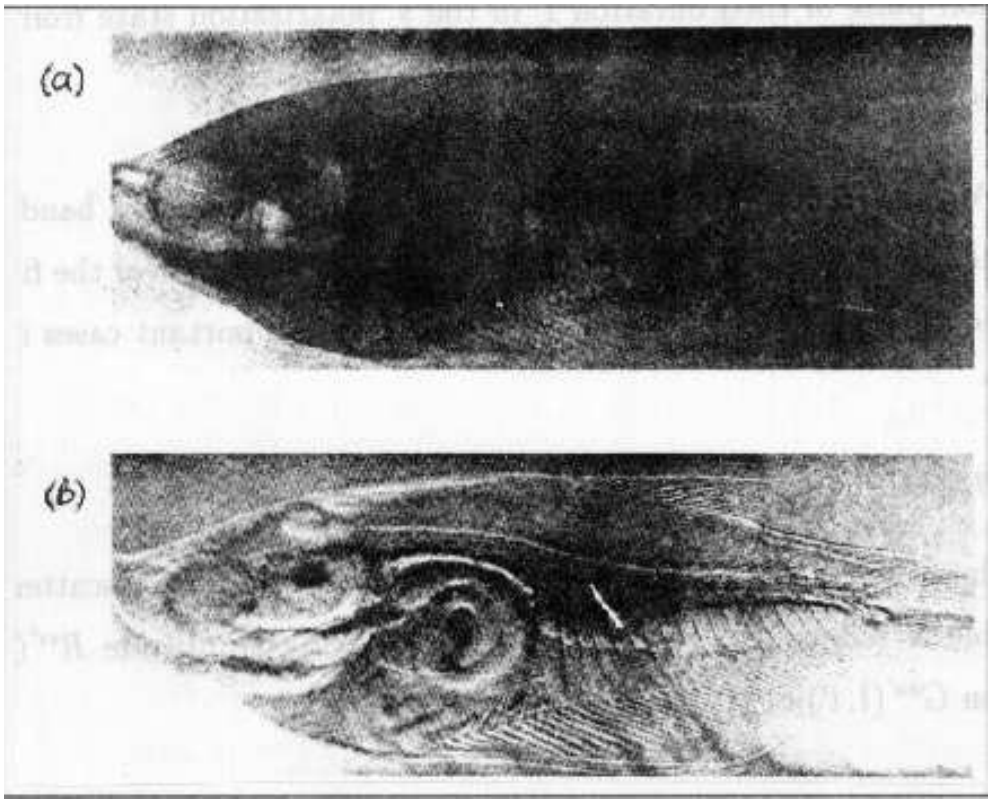

FIG. 7. The image of aquarium fish, top figure is an absorption contrast, bottom figure is PDI (phase dispersive image)

used in monochromators, and the asymmetry factors were $b_1 = 0.4$ and $b_2 = 0.07$ for Mo K_α. Under these conditions the authors estimate the longitudinal coherence length as 33 ± 3 μm and transverse coherence length as 175 ± 16 μm. The accurate theoretical analysis of the mechanism of image formation is absent in the paper (in these lectures it will be done later). However, the authors give some qualitative estimation. The image is formed due to a deviation of rays scattered by inhomogeneous object from the initial direction. The deviation angle $\gamma = (\delta_1 - \delta_2) \tan \alpha$ where δ_1 and δ_2 are decrements of refractive indexes and α is the angle between the primary beam direction and the normal to the boundary between two media. High angular sensitive analyzer reveals these inhomogeneous deviations. Therefore the contrast can be divided on "area contrast" where α is less apparently then $\pi/2$ and "boundary contrast" where α is close to $\pi/2$.

To obtain the better contrast one has to use a Laue diffraction in an analyzer and to move the working point from the maximum of reflection curve to the point where the slope of rocking curve has maximum value. One of the bright result of this group is the image of aquarium fish shown in Fig. 7. The maximum thickness of fish was 5 mm. The top image (a) is obtained when the analyzer was moved out of the Bragg position. Therefore this image is angular insensitive and it shows only a shadow of high density parts of object (vertebral spine and ribs) due to stronger absorption The bottom image (b) is just the PDI (phase dispersion image) in reflected beam. Here one can to distinguish the brain, pectoral fin and air bladder walls as well as the mouth and an inguested worm. Despite the bright image the qualitative estimations are impossible because this technique today does not allows to measure a phase shift accurately. Moreover, the character of image depends significantly on the working point on the rocking curve.

6.3 Demonstration of phase-contrast X-ray computed tomography using an X-ray interferometer

The X-ray interferometry exists more than three decade after the first realization by

- U. Bonse and M. Hart, Appl. Phys. Lett. 1965, vol. 6, p. 155.

The LLL interferometer consists of three blocks of the same crystal having the parallel surfaces. The Laue (transmission) case of diffraction is used. First block is called a splitter (S) because it divides one incident beam on two beams - transmitted and reflected. In symmetrical experimental scheme and at the exact Bragg position of the crystal the intensity of both waves are equal each other. The second crystal is called mirror (M) because here each beam is divided on two beams once again. In this process the double reflected beam becomes directed along the incident beam and it goes for intersection with the beam reflected in the second crystal only. The third crystal is called analyser (A) because it is placed just at the region of intersection of these two beams.

First applications of this device were connected with the observation of the lattice deformations in the crystal-analyzer. Indeed, the two intersecting beams form a standing wave which has a period of the crystal lattice of first two blocks. If the crystal lattice of third block is slightly different due to small rotation or stress then in some part of the crystal the nodes of standing wave will coincide with the atom positions while in another parts these will be just between them. The reflection and transmission in these regions will be rather different giving the picture of black white strips (moire pattern). However, if

the crystal-analyzer will have a perfect crystal lattice then the transmission and reflection will be homogeneous in space. Now to make the image one can place in the path of one ray some inhomogeneous object which will make shift of the phase inhomogeneously. The simplest object is a wedge. In this case the phase shift is homogeneous so we obtain the set of interference fringes of equal thickness and equal distance between them.

The next step is to place in addition the inhomogeneous object which will distort the order of initial fringes. The shift of fringes just will show directly the phase shift produced by object. This simple idea was realized only recently by A. Momose from Hitachi firm (Japan). First results were published in

- A. Momose, Nucl. Instr. Meth. 1995, vol. A352, p. 622.

The method of direct phase shift measurement was used for the Phase-contrast X-ray computed tomography (PCX-CT). Each measurement allows to obtain the map of phase shift which is proportional to an integral over path of X-ray beam decrement of refractive index. So this map may be considered as a projection of object along the path of X-ray beam. Rotating the object one can obtain a set of such projections. Then the standard technique of computed tomography allows to restore the distribution of the electronic density inside the object.

The experimental setup of Momose technique is shown in Fig.8. 220 diffraction and Silicon crystals were used for both the monochromator and the interferometer. Despite the phase shift is visible directly on the interference pattern to obtain the accurate value of the phase shift one needs to apply a Fourier Transformation Method which allows us to eliminate the carrier fringes.

The simple method of measuring is restricted by the value of phase shift less than 2π. However, the method can be extended to overcome this restriction if one is able to measure a set of fringes pattern each is obtained with the shift of the wedge on the value d/M compared to the initial position where d is a distance between fringes. The theory is very simple therefore we consider it directly below. So we have the intensity which spatial dependence consists of the fringes of carrier frequency f_0. The middle value $a(x,y)$ as well as the amplitude of oscillations $b(x,y)$ (contrast) and phase shift $\varphi(x,y)$ produced by object are slow functions on the period $d = 1/f_0$ (carrier fringe interval)

$$I(x,y) = a(x,y) + b(x,y)\cos\left(2\pi f_0 x + \varphi(x,y)\right). \tag{40}$$

where we suppose the fringes to be parallel to y-axis. Let us represent the cosine function through the exponentials

$$I(x,y) = a(x,y) + c(x,y)\exp\left(2\pi i f_0 x\right) + c^*(x,y)\exp\left(-2\pi i f_0 x\right). \tag{41}$$

where

$$c(x,y) = \frac{1}{2} b(x,y)\exp\left[i\varphi(x,y)\right] \tag{42}$$

is a slow complex function compared to exponential of carrier frequency.

Now it is clear that the Fourier spectrum of such a function has a shape of three sharp peaks divided by relatively large distance between them

$$I_F(f,y) = a_F(f,y) + c_F(f - f_0, y) + c_F^*(f + f_0, y). \tag{43}$$

The left and right peaks, corresponding to second and third terms of Eq.(43), just contain the information about the phase shift. Taking, for example, the right peak (the second term) and making the reverse Fourier transformation one then obtains the phase shift directly from Eq.(42) as an imaginary part of $\log[c\,(x,y)]$. This method is just restricted by the value 2π of the phase shift.

Another method allows to work with a set of patterns each of them is described by the formula

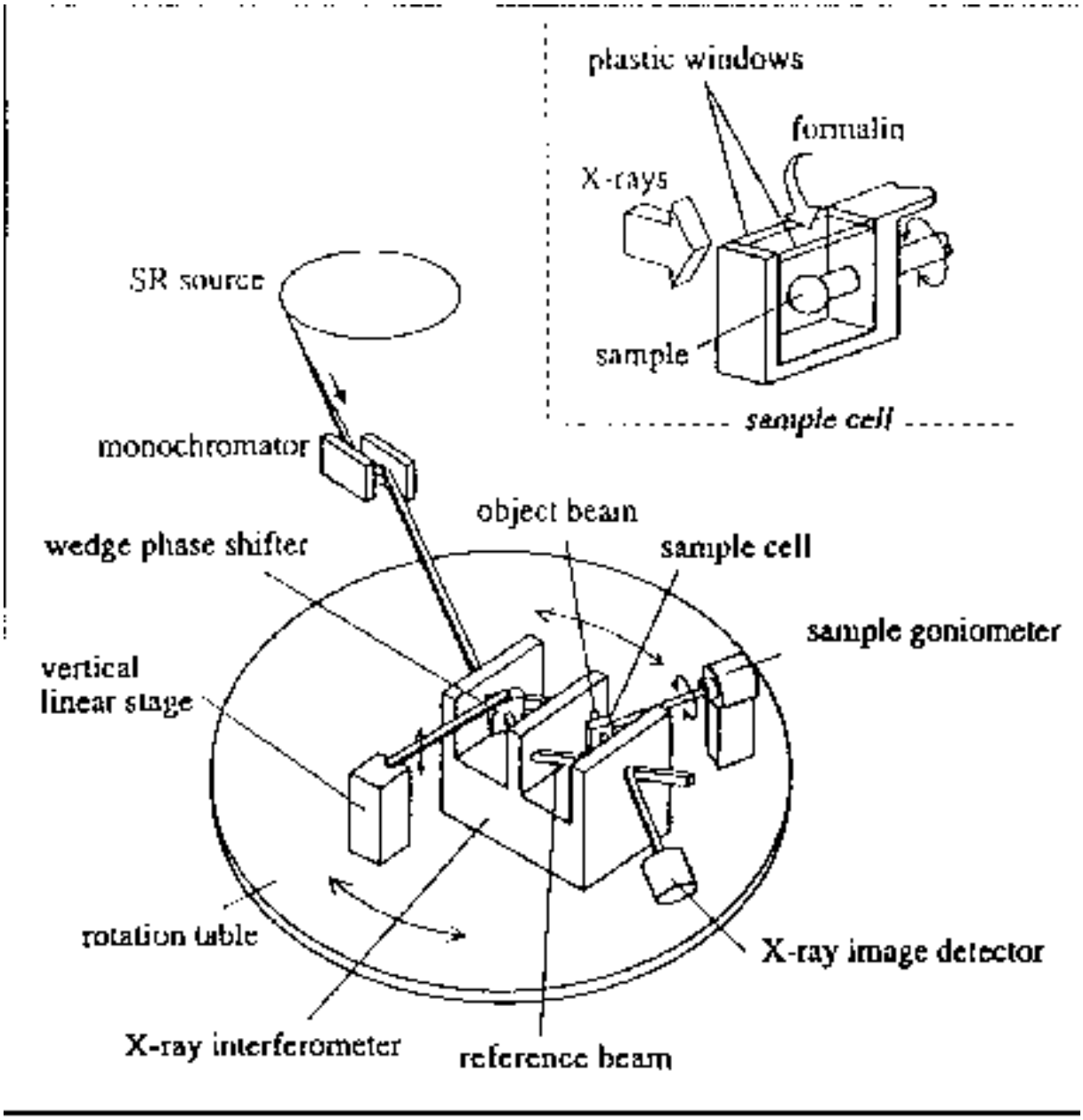

FIG. 8. The experimental setup of Momose technique

$$I(x,y;N) = a(x,y) + b(x,y)\cos\left(2\pi f_0 x + 2\pi\frac{N}{M} + \varphi(x,y)\right). \tag{44}$$

The summation of all patterns with the weight $\exp(-2\pi iN/M)$ allows us to kill the middle value and the left peak of Fourier transformation. As a result we obtain

$$\sum_{N=1}^{M} I(x,y;N)\exp\left(-2\pi i\frac{N}{M}\right) = \frac{1}{2}Mb(x,y)\exp\left[2\pi i f_0 x + i\varphi(x,y)\right] \tag{45}$$

Now we may extract the phase shift from the imaginary part of logarithm because the carrier frequency is known. This method is more difficult and in addition it is restricted essentially by detector resolution. Fig.9 shows the raw data of experimental measurement when the object was a plastic sphere. The top figure shows the results of experiment when the plastic sphere exposed in air. One can see the carrier interference fringes the shadow of the rod which keeps the object (at the right) and the shadow of the object itself. Only a new set of interference fringes of very small distance appears in the centre of the object shadow. The reason is that the phase shift produced by object is very large compared to 2π and very quickly changes near the boundary of the sphere. Therefore the method described above is unapplicable for this object. In terms of Ingal and Beliaevskaya group this method is able to measure only the "area" image while the "boundary" image cannot be measured.

To solve the problem of strong refraction near the boundary the object was placed in water. This allows to decrease the difference of decrement of refractive index near the boundary. The bottom figure shows the result of measurement in this case. Here the object shadow disappears and instead one can clearly see the inhomogeneous shift of carrier interference fringes.

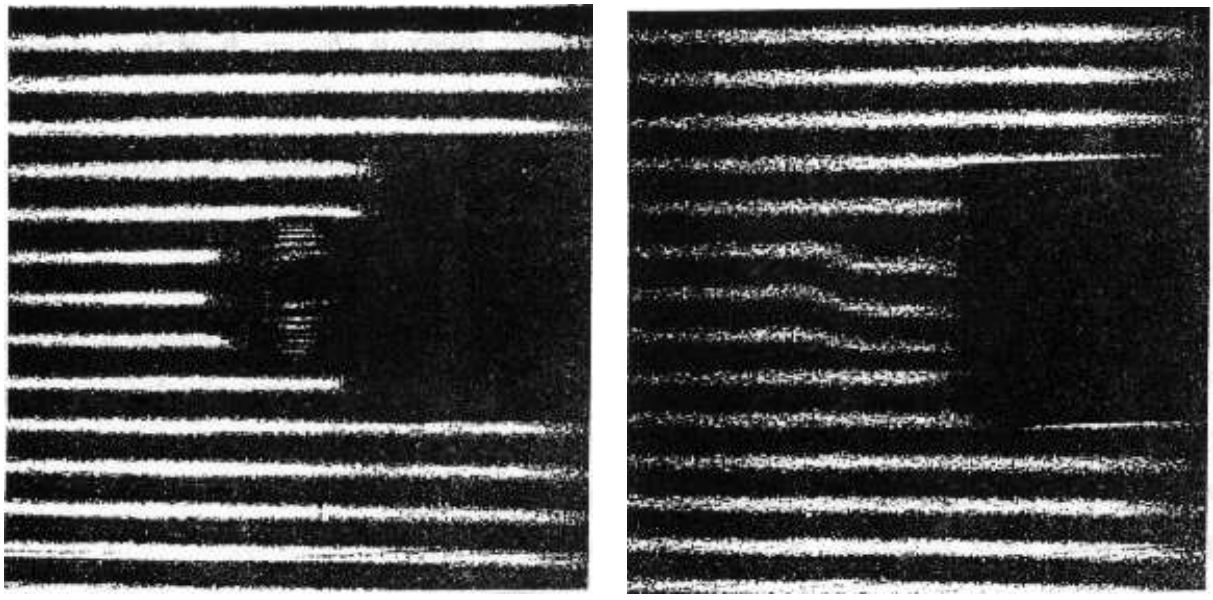

FIG. 9. The interference pattern of plastic sphere in air (left) and in water (right)

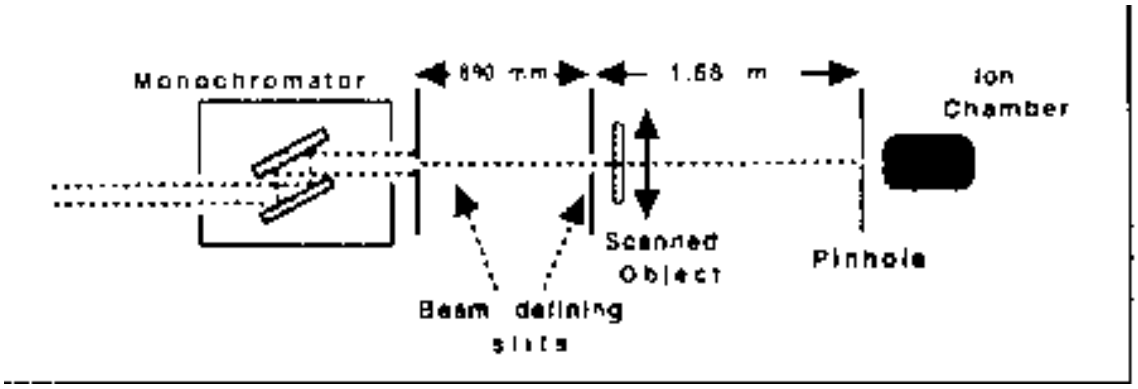

FIG. 10. The experimental setup of Australian group

6.4 Quantitative Phase Imaging Using Hard X Rays

The method of X-ray phase imaging which is based on traditional optical ideas of studying the inhomogeneous medium is developed recent years also in Australia. The first experimental result was presented by group of researches: K. A. Nugent, T. E. Gureyev, D. F. Cookson, D. Paganin, Z. Barnea from Melbourne in the publication

- Phys. Rev. Lett., 1996, vol. 77, p. 2961.

They use the experimental arrangement similar to set-up of in-line holography used by Snigirev's group at ESRF (see below). However, the method of registration of the inhomogeneous intensity suppose the procedure of averaging over large enough area together with a possibility to make a good quantitative recording (ion chamber with a pinhole in front).

The theoretical foundation of the approach was developed in the main part by Gureyev (former Russian scientist from Russian Snigirev's group in Chernogolovka). The approach is based on the idea that the pure transparent object produces the inhomogeneous phase shift of the wave which transforms to the inhomogeneous intensity distribution at the definite distance from the object. The latter (being represented in smoothed state) can be described in an approximation of transport of intensity equation. This equation can be obtained directly from Maxwell's equation for a scalar wave field in the form (see above)

$$E(x,y,z) = I^{1/2}(x,y,z)\exp\{ikz + i\varphi(x,y,z)\} \tag{46}$$

where $k = 2\pi/\lambda$ is a wave number of X-rays. The intensity $I(x,y,z)$ and the phase shift $\varphi(x,y,z)$ are assumed to be slowly varying functions obtained by means of some smoothing procedure, for example. Under this condition the transport of intensity equation can be derived directly from the Maxwell's equation which has the form

$$k\frac{\partial I(x,y,z)}{\partial z} = -\nabla_\perp\left[I(x,y,z)\nabla_\perp\varphi(x,y,z)\right], \qquad \nabla_\perp = (\frac{\partial}{\partial x}, \frac{\partial}{\partial y}) \tag{47}$$

which just determines the mechanism of transformation of the phase inhomogeneity to the intensity inhomogeneity.

The method of solution of this equation is proposed and is tested on a model object as a commercial carbon electron microscope calibration grid with a period of 330 μm and of 68$\pm$24 μm thickness. The experiment was performed with 16 keV X-rays at beam line 20A (Australian) at the Photon Factory (KEK, Tsukuba, Japan). The experimental set-up is shown in Fig.10. The divergence of X-ray beam was approximately 0.38 mrad horizontally and 0.037 mrad vertically. Two 100 μm square aperture were placed to produce a uniform beam with a square profile and to decrease the effective source size for increasing the spatial coherence. The initial experimental data (intensity) have a correct periodicity (see Fig.11 (left)). To obtain the phase image from the intensity the procedure of solving the transport of intensity equation by means double Fourier transformation and filtering the data was used. The result of phase shift reconstruction is shown in Fig.11 (right). The obtained quantity of the phase shift was compared with an independent determination from the absorption of 8.05 keV X rays with a good agreement. The method is rather simple and is in close connection with the ideas of holographic reconstruction under near field conditions (see below). The most fresh paper of this group has been arrived few days ago

- D. Paganin, K. A. Nugent, Phys. Rev. Lett., 1998, vol. 80, p. 2586.

All other references can be found in this paper.

6.5 Phase Contrast Microimaging by Coherent High Energy Synchrotron Radiation in experimental set-up of in-line holography

This approach is developed by A. Snigirev's group at beamline ID24 of ESRF which includes I. Snigireva, A. Souvorov, C. Raven, F. Legrand, V. Kohn, S. Kuznetsov and

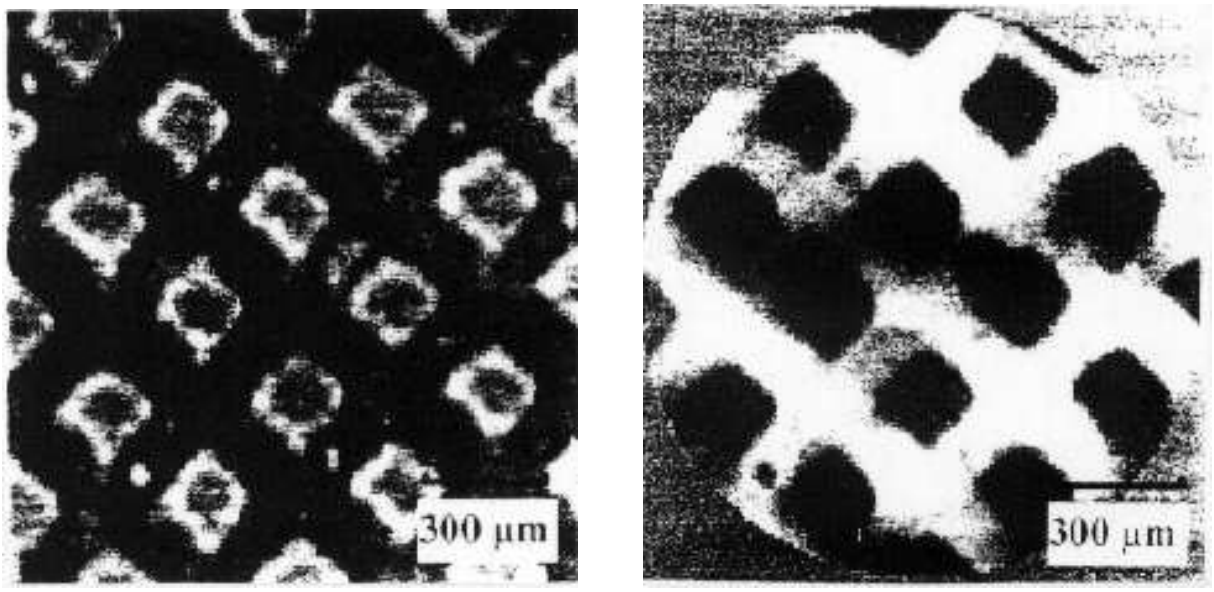

FIG. 11. The raw data of intensity distribution(left) and the reconstructed profile of phase shift(right)

others. First results were published in:

- ESRF Newsletters, 1995, June, No. 24, p. 23
- Rev. Sci. Instrum., 1995, vol. 66, December, No. 12, p. 5486.

Schematic display of the experimental set-up is shown in Fig.12 where a distance from the source to the object is from 30 to 60 m and the distance from the object to the high resolution spatial detector (CCD camera or a film) is varied from 0.2 to 2 m. Only a monochromator is needed to provide a temporal coherence of the radiation while the spatial coherence is rather good taking into account that the size of source is only 30 μm.

This scheme allows to obtain the images of small objects or small details of large object of quite different type in dependence on the distance from the object to the detector. At very small distance the image is formed by absorption contrast where only a shadow of high absorbing parts of object has smaller intensity. At small distance a boundary contrast appears as a result of interference of strongly scattered rays at the boundary due to refraction with the reference rays. This effect is a coherent effect and it leads to a change of intensity up to 100 per cent and higher. Therefore the boundaries of different parts of the object becomes visible clearly even for pure transparent object. The authors named such an image as outline image. The comparison of absorption image and outline image is shown in Fig.13 where an image of dry seaweed Valonia ventricosa at E = 20 keV registered just after the sample (left) and at 5.5 cm distance (right). One can see the great difference of quality of images based on the phase shift and on the absorption. The outline image in this scheme is not a parasitic effect as in all schemes considered above: (1) with perfect crystals, (2) based on the interferometer or (3) using the transport of intensity equation for the reconstruction. Just the outline imaging has a simplest nature and it is easy to understand. This technique allows to obtain the images of high quality. An an example, one can see in Fig.14 the outline image of knee of mosquito long leg. The thickness of hairs is about 10 μm, however even the structure of hairs (inhomogeneous thickness along the hair) can be distinguished.

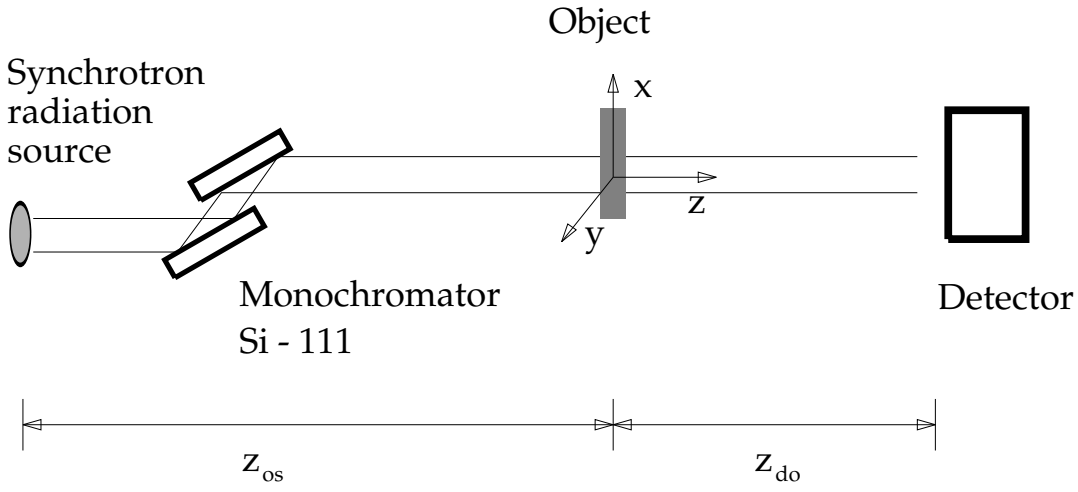

FIG. 12. The simple scheme of experiment with coherent synchrotron radiation, see text

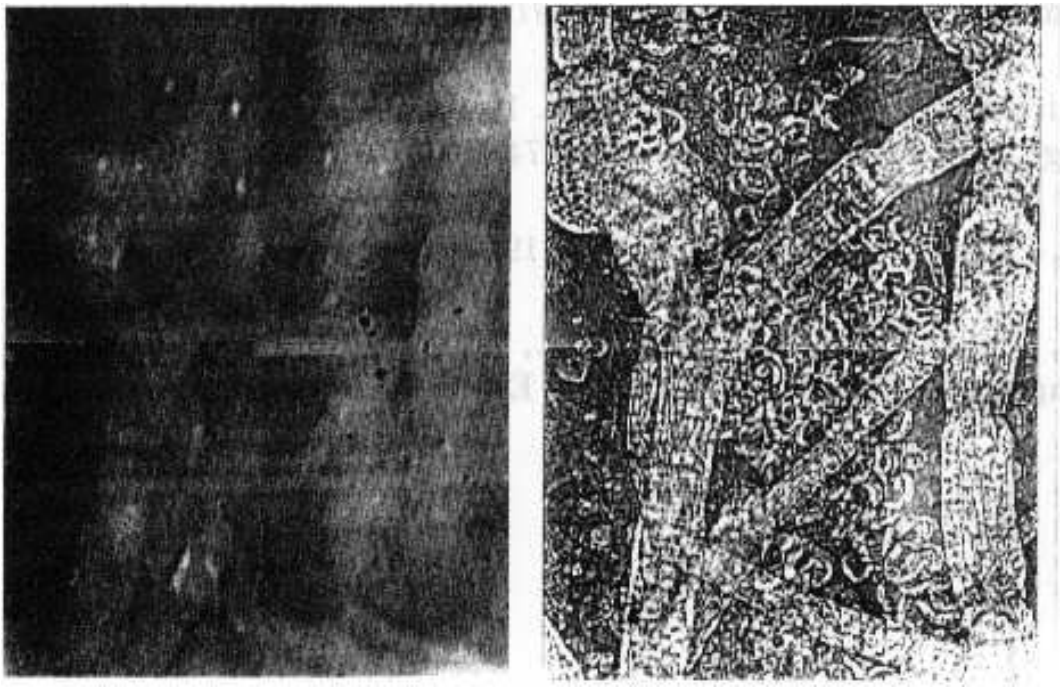

FIG. 13. The comparison of absorption image of dry seaveed Valonia ventricosa (left) and outline coherent image (right)

As for "area contrast", it also can be measured. However, in this case the interpretation is not direct. In addition, the open character of this scheme leads to a situation when

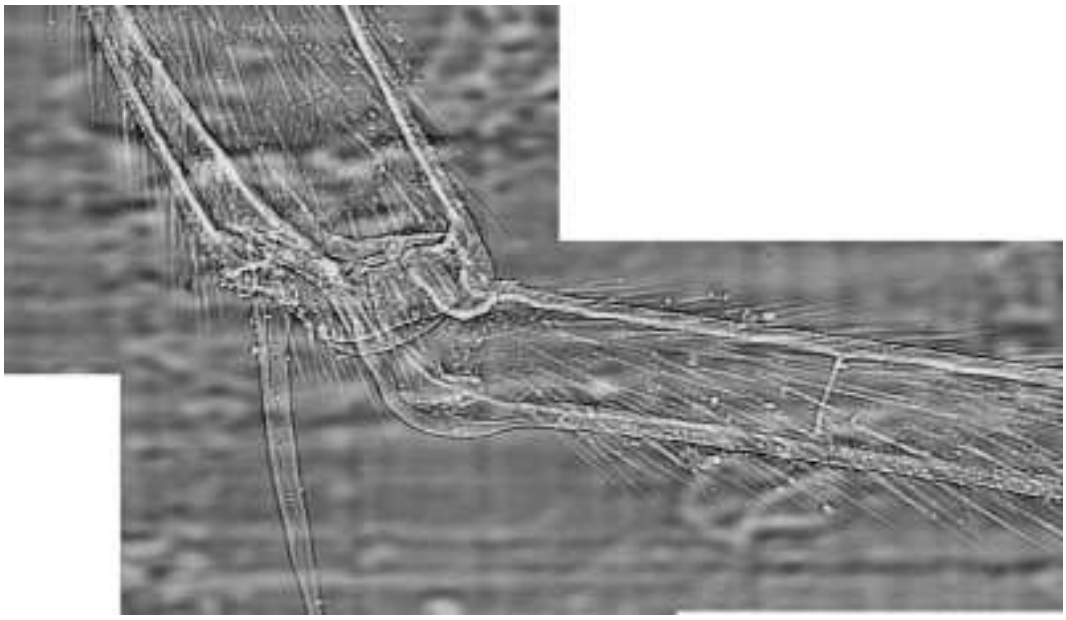

FIG. 14. The outline image of knee of mosquito long leg

just the area contrast gives, as a rule, the parasitic image, created by all objects on the path of X-rays and not only by the sample. For example, in Fig.14 one can see the inhomogeneous background caused by beryllium foil of inhomogeneous thickness at the window of synchrotron radiation beam line. As it was demonstrated on series of different objects the outline imaging allows to make the tomography reconstruction of the boundaries inside the object. The first results are published in

- C. Raven, A. Snigirev, A. Koch, I. Snigireva, V. Kohn,
  . Proceedings of SPIE, 1997, vol. 3149, p. 140.

The experimental scheme used in this technique is vary similar to the well known in-line (Gabor) holographic scheme used in optics with laser light source. However, the difference in 10^{-4} between the wave length value in visible light optics and X-rays optics does not allow to explore the methods of reconstruction of the phase from intensity which used in visible light optics. Therefore only the methods applicable to near field condition may be used. One of them is just the method of equation of transport of intensity. However, there may be modifications. The theory will be considered in the next sections.

7. THE THEORY OF PLANE WAVE IMAGING

Let us try now to understand theoretically what we see on the X-ray images of non-crystalline objects. All approaches presented above may be divided on three essentially different directions which are based on the different experimental equipments and therefore have different application domains. Let us call the first direction "imaging in the plane wave topography scheme" or more shortly "plane wave imaging", the second direction "interferometric imaging" and third direction "imaging in the in-line holography scheme" or more simply "in-line imaging". All directions are developing today rapidly. However, there appeared only few theoretical works were some aspects of the problem are examined. The complete understanding of all possibilities and restrictions of described above techniques are absent.

The plane wave imaging scheme, in principle, does not demand a coherent source of X-rays because if one uses a quasi-monochromatic radiation of X-ray tube then the monochromator serves as a collimator which restricts the angular width $\Delta\theta$ of the incident beam by the value $\Delta\theta = (\Delta\lambda/\lambda)\tan\theta_B$ according to the Bragg law where $(\Delta\lambda/\lambda)$ is a relative width of the spectral line used in the experiment (usually about $2\cdot 10^{-4}$). Conditionally we may consider the incident wave as a plane wave. The role of real divergence of the incident wave is not studied up to now. However, as the first approximation it is good to average the intensity over the angular width $\Delta\theta$ of the incident radiation. The plane wave can be approximated by a set of parallel rays which go through the object. Owing to a refraction on the boundary between the media with different refraction index each ray changes its direction of propagation. The angle of deviation is so small that the space distribution of intensity cannot be resolved by conventional detectors. The Bragg diffraction in the crystal analyzer is just used for a registration of these small changes of ray direction.

Such a simple interpretation of physical principles of plane wave imaging given usually by experimentators is inconvenient for the theory. First of all, it is clear that two-beam diffraction cannot resolve the angular inclinations in the vertical plane normal to the

scattering plane. The resolution arises only in the scattering plane containing the wave vectors of incident and diffracted waves. On the other hand, the accurate theoretical consideration must be performed in terms of inhomogeneous wave field and the propagators of the two-beam diffraction. This is the standard approach of X-ray topography of crystal lattice defects. Today only two theoretical papers are published on this topic

- V. A. Bushuev, V. N. Ingal, E. A. Beliaevskaya,
  . Kristallografia, 1996, vol. 41, p. 808 (in Russian)
- T. E. Gureyev and S. W. Wilkins, Nuovo Cimento, 1997, vol. 19D, p. 545

where just this approach was considered.

Thus, let us assume first that the object is illuminated by the plane wave along the reference direction (we may call it the optical axis or z-axis). The wave field after the object has the form (see above)

$$E_0(x,y,z_1) = \exp\left(i\Phi(x,y)\right)\exp\left(-M(x,y)\right) \tag{48}$$

where

$$\Phi(x,y) = \frac{2\pi}{\lambda}\int_{z_0}^{z_1} dz'\,\delta(x,y,z'), \qquad M(x,y) = \frac{2\pi}{\lambda}\int_{z_0}^{z_1} dz'\,\beta(x,y,z'). \tag{49}$$

Here δ is an inhomogeneous decrement of refractive index which is proportional to the local electronic density of matter while β is an index of absorption. In general the wave field has variable the phase and the amplitude therefore the contrast is mixed: refraction-absorption contrast.

When the distance from the object to the crystal-analyzer is small enough, we may neglect the z-dependence of the field and assume that the same field falls on the entrance surface of the crystal analyzer. The detector measures the wave field scattered by the crystal-analyzer. The result will depend on the case of diffraction (Laue or Bragg) and on the type of the beam (transmitted or reflected). Let us consider the reflected beam. The problem may be formulated in terms of the propagator functions considered above. Taking into account the rotation of coordinate system at the crystal analyzer (the z-axis along the normal to the surface) we have at the exit surface of the crystal

$$E_h(x,y) = \int dx' P_{h0}(x-x',\alpha)\exp\left(i\Phi(cx',y)\right)\exp\left(-M(cx',y)\right) \tag{50}$$

where $c = \cos\varphi$, φ is an angle of rotation of the z-axis, and the explicit expression for the propagator depends on the case of diffraction (Laue or Bragg). We assume that the scattering plane is (x,z) plane. The parameter $\alpha = -2\sin 2\theta_B \Delta\theta_c$ shows in explicit form the dependence of the propagator on the angular position of crystal-analyzer relative to the exact Bragg position. The index c just points on the crystal.

One can see that the y-coordinate enters in the formula as a parameter. This means that the crystal-analyzer can resolve the phase inhomogeneity along the y-axis only in the sense of y-dependence of x-axis inhomogeneity. Let us estimate the frame of applicability of "ray inclination" approximation. As it follows from the Eqs.(35) and (38) the spatial dependence of the propagator function is rather inhomogeneous. In the Bragg case this region does not depend on the crystal thickness (in the case of thick crystal) and can be estimated as not more than

$$\Delta_x = \frac{\lambda \cos\theta_B}{\pi |\chi_h|} = L_{ex} \mathrm{ctg}\, \theta_B \tag{51}$$

where L_{ex} is an extinction length of the plane wave theory. Let us assume that the real part (Φ) and imaginary part (M) of the phase of wave field ($\Psi = \Phi + iM$) can be expanded in the Fourier series

$$\Psi(cx') = \Psi(cx) + \frac{d\Psi}{dx} c(x' - x) + \frac{d^2\Psi}{2dx^2} c^2 (x' - x)^2 + \cdots, \quad \frac{d\Psi}{dx} c = \frac{2\pi}{\lambda} c \Delta\theta_x \tag{52}$$

where the parameter $c = \sin\theta_B$ ($\varphi = \pi/2 - \theta_B$) in the Bragg case and $\Delta\theta_x$ is the deviation of the ray at x-coordinate in the positive direction of the x-axis.

Let us assume moreover that we can neglect the second and higher derivatives of the phase inside the region of width Δ_x (see Eq.(51),.namely,

$$\frac{d^2\Psi}{dx^2} c^2 \Delta_x^2 + \cdots < 1 \tag{53}$$

Then the integral of the propagator with the exponential can be calculated analytically and we obtain the result as

$$E_h(x, y) = \exp\left(i\Phi(cx, y)\right) \exp\left(-M(cx, y)\right)\ r(\Delta\theta_c - \Delta\theta_x), \tag{54}$$

where

$$r(\Delta\theta) = i \frac{\chi_h}{y + \sqrt{y^2 - \chi_h^2}}, \quad y = \chi_0 + \sin 2\theta_B\, \Delta\theta \tag{55}$$

is a usual reflection amplitude of plane wave. However, now it depends on the local ray deviation through the local dependence on the first derivative of the phase shift. We note that the gradient of absorption also enters here as an imaginary part of the $\Delta\theta_x$ value.

The intensity registered by position sensitive detector equals

$$I_h(x, y, \Delta\theta_c) = \exp\left(-2M(cx, y)\right)\ |r(\Delta\theta_c - \Delta\theta_x)|^2 \tag{56}$$

So we see that the crystal-analyzers cannot reveal the local phase shift but it can reveal the local phase shift gradient through the high sensitivity of the reflectivity of the crystal-analyzer. In the case of finite angular width of the incident radiation the registered really intensity is

$$J_h(x, y, \Delta\theta_c) = \left(\sum_s \int d\theta' W_s(\theta') \right)^{-1} \sum_s \int d\theta' I_h^{(s)}(x, y, \Delta\theta_c + \theta') W_s(\theta') \tag{57}$$

where $W_s(\theta)$ is the function describing an angular divergence of the incident beam and summation is assumed on two polarization states.

The condition (53) means that we may apply the plane wave theory (the ray approximation) only in the analysis of the "area contrast" with a slow change of the refractive index. However, even in this case the interpretation of the image and the reconstruction of the phase is not so simple. First of all, the image depends significantly on the base

angular point on the "rocking curve" of the crystal analyzer. The most suitable point is at the side of the reflectivity maximum. Then the different values of the ray direction will be represented as a map (only in x-direction) of different gray levels. It is known (see Fig.15(left)) that the angular width of such a region of high angular sensitivity on the rocking curve is limited. Therefore all regions where the gradient of the phase leads to the angular shift which exceeds this region will be shown in distorted form.

On the other hand, the regions where the condition (53) is not fulfilled will be also shown in the image. However, the origin of this image will be different from the picture of ray inclination distribution. It can be analyzed qualitatively or calculated quantitatively using the accurate expression (50). In the paper of Gureyev and Wilkins two another limiting cases are considered. First, when the phase shift is a rapid function of x and, second, the stepwise character of the pure phase shift (without an absorption). Despite the fact that the approximate analytical formulas can be obtained the understanding stays on the low level. So the problem here is only under solution.

Mechanism of the contrast formation in the Laue case of diffraction is more complicated because the propagator has more complex structure. In addition it depends on the crystal thickness. As it was shown above the propagator has the structure of the product of pure exponential function and the Bessel function $\mathrm{J}_0(x)$, namely,

$$P_{h0}(x,d,\alpha) = \frac{i}{2}B\exp\left(\frac{i\pi}{2\lambda\sin\theta_B}\left[(2\chi_0-\alpha)x_d+\alpha x\right]\right)\ \mathrm{J}_0\left(B\sqrt{x_d^2-x^2}\right), \tag{58}$$

where

$$x_d = d\tan\theta_B, \quad B = \frac{\pi\chi_h}{\lambda\sin\theta_B}, \tag{59}$$

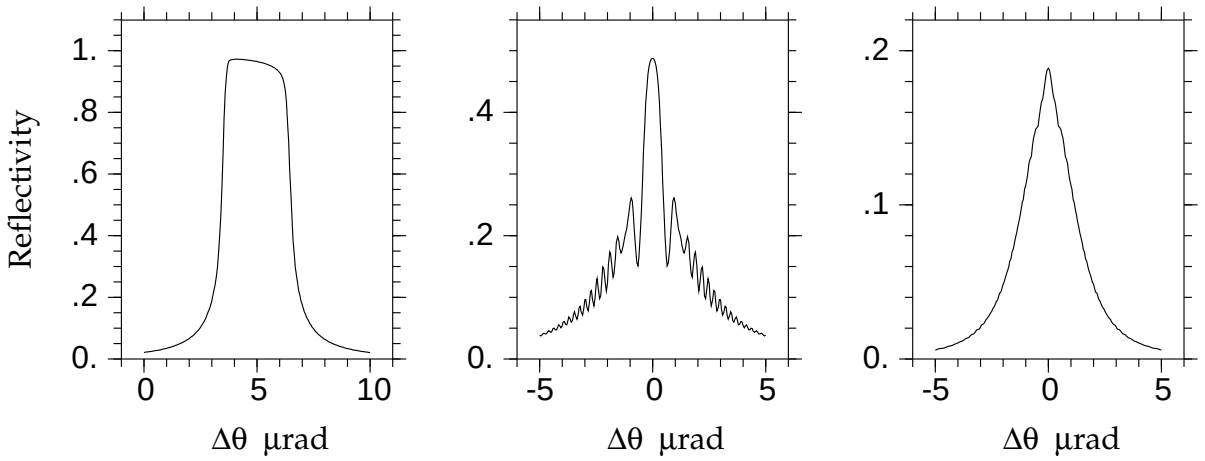

FIG. 15. Reflectivity of Silicon crystal analyzer for X-rays of Mo K_α energy ($\lambda = 0.709$ Åfor three cases: (left) 511 reflection, Bragg case; (middle) 422 reflection, Laue case, crystal thickness $d = 564$ μ; (right) 422 reflection, Laue case, $d = 2135$ μm. The incident beam is assumed to be sigma polarized and having the angular divergence 0.2 μrad and the Gaussian shape of angular distribution

d is the crystal thickness and the symmetrical case of diffraction is assumed. Let us consider two limiting cases of crystal analyzers thickness. In the case of thin crystal we may neglect the absorption of X-rays in the crystal. Then the Bessel function has the maximum value for zero argument when $x = \pm x_d$. Taking into account the expression (50) we may conclude that the rays which undergo only one reflection gives the maximum contribution, i. e., for the point x on the exit surface the small regions near the points

$$x' = x \pm x_d \tag{60}$$

on the entrance surface are the more essential. This effect is well known in the theory of X-ray topography as the "margin effect".

Once again we may assume that the complex phase shift produced by the object can be expanded in the Fourier series and only the first derivative of the phase is essential. However, now the region Δ_x is the basis of the Borrmann delta $\Delta_x = 2x_d$ and it depends on the crystal thickness. The amplitude of the reflected beam equals in this approximation

$$E_h(x,y) = \exp\left(i\Phi(cx,y)\right)\exp\left(-M(cx,y)\right)\, r(\Delta\theta_c + \Delta\theta_x, d) \tag{61}$$

where

$$r(\Delta\theta, d) = i\exp\left(\frac{i\pi x_d}{2\lambda\sin\theta_B}(2\chi_0 - \alpha)\right)\frac{\sin(s_\alpha B x_d)}{s_\alpha},$$
$$s_\alpha = \sqrt{1 + (\alpha/2\chi_h)^2}, \qquad \alpha = -2\sin 2\theta_B\,\Delta\theta. \tag{62}$$

The angular properties of thin crystal analyzer in the Laue case is different from the Bragg case (see Fig.15(middle)). The region of maximum has no sharp boundaries. However, the additional extinction oscillations appears there due to an existence of two waves with slightly different velocity. The slope of the rocking curve at the boundary of the central peak may be high enough that increases the angular sensitivity. The absence of large region of approximately constant reflectivity allows to avoid the arfifacts. On the other hand, the interpretation of the image for objects having parts with different level of the density inhomogeneity becomes also not simple. The margin effect may be used but up to now it is not made.

In the case of thick crystal when the absorption is essential the Bessel function becomes growing function and it reaches the maximum value for maximum argument, therefore for the point x on the exit surface the region near the point $x' = x$ on the entrance surface is essential and the width Δ_x is the decreasing function of the crystal thickness. For rather thick crystal the image reveal local first and second derivatives of the phase. If the second derivative is small then the approximation of ray inclination can be also used. The angular dependence in this case is not so sharp (see Fig.15(right)) however it is still suitable. For my opinion the thick crystal analyzer must be considered because it leads to high local sensitivity. However in the paper of Bushuev et al., cited above only the case of thin crystal is accepted and an analysis of all possibilities of the method is absent. Only the numerical computer simulation of some particular cases is made. The comparison of the experimental results of Ingal and Beliaevskaya with the calculations shows good coincidence. Nevertheless, this case needs in the following development of the theory.

8. THE THEORY OF IN-LINE IMAGING

8.1 The propagator and the problem of coherence

The experimental set-up of in-line imaging (see Fig.12) can be examined in two steps. On the first step we may assume that the source of the radiation has no size (the point source) which produces the spherical wave. The existence of the monochromator allows us to consider the monochromatic spherical wave. Because the distances along the optical axis (z-axis) is very large compared to transverse distances the small angle approximation can be used with a good accuracy. At the second step we need to take into account the real size of the source and to estimate how it influence the image. As it will be shown below, in the case of in-line imaging the pattern of point source image has to be averaged over the projection of source size on the image plane. For this purpose we shall consider the arbitrary coordinates (x_s, y_s) of the point source. The wave field in the plane (x, y) normal to the optical axis just after the object can be written as

$$E(x, y, z_o) = E_0(x - x_s, y - y_s, z_{os}) \exp\left(i\Phi(x, y)\right) \exp\left(-M(x, y)\right) \tag{63}$$

where

$$E_0(x, y, z) = \frac{1}{z} \exp\left(iK\left[z + \frac{x^2 + y^2}{2z}\right]\right) = \exp(iKz) S(x, z) S(y, z) \tag{64}$$

is the spherical wave in a small angle approximation, $K = 2\pi/\lambda$, z_o is the absolute coordinate of the plane just after the object, $z_{os} = z_o - z_s$ is the distance source-to-object, and $S(x, z)$ is the partial transverse component of the spherical wave which is defined as

$$S(x, z) = \frac{1}{\sqrt{z}} \exp\left(iK\frac{x^2}{2z}\right). \tag{65}$$

Let us consider the situation when the distance from the object to the detector $z_{do} = z_d - z_o$ is significant in the sense that the approximation of simple transition of wave field to the detector plane and even the approximation of geometrical optics is not valid. In this case we need to solve the Maxwell's equation in empty space between the object and the detector. Taking into account the Huygens-Fresnel principle the solution may be expressed in terms of Kirchhoff integral over the total plane (x, y) after the object normal to the optical axis

$$E(x_d, y_d, z_d) = \int dx \int dy\, P_t(x_d - x, y_d - y, z_{do}) E_0(x, y, z_o) \tag{66}$$

where $P_t(x, y, z)$ is the propagator of x, y-distribution of the wave field along the z-axis. The accurate propagator is proportional to the spherical wave. However we can use a small angle approximation once again. It allows us to express separately x and y dependence of the propagator as follows

$$P_t(x, y, z) = \exp(iKz) P(x, z) P(y, z), \tag{67}$$

where

$$P(x,z) = \frac{1}{\sqrt{i\lambda z}} \exp\left(iK\frac{x^2}{2z}\right) = \frac{1}{\sqrt{i\lambda}} S(x,z) \tag{68}$$

In general case the integral 66 will transform the phase shift distribution $\Phi(x,y)$ produced by object in the new wave field distribution which will lead to the inhomogeneous intensity distribution - the value which can be measured by the detector. The character of this transformation of the phase to the intensity depends on the properties of the propagator. The propagator of in-line scheme is essentially two-dimensional one as against the plane wave scheme considered above. However, to simplify the problem we consider first the model object which gives only one-dimensional distribution of the phase shift, for example, only along the x-axis. Such an object - the round Boron fiber with Tungsten round core - really was investigated intensively in in-line scheme. Since the object changes the wave field only in the x-direction we can calculate the integral over y directly. The result looks as a convolution of two propagators which equals the propagator once again but on the total distance

$$\sqrt{i\lambda}\int dy P(y_d - y, z_{do}) P(y - y_s, z_{os}) = \sqrt{i\lambda} P(y_d - y_s, z_{ds}) \tag{69}$$

where $z_{ds} = z_{do} + z_{os} = z_d - z_s$ is the source-to-detector distance. This result is well known and it has a clear physical sense from the point of view of Huygens-Fresnel principle. Thus we obtain the expression

$$E(x_d, y_d, z_d) = \exp(iKz_{ds}) S(y_d - y_s, z_{ds}) \int dx P(x_d - x, z_{do}) S(x - x_s, z_{os}) F(x) \tag{70}$$

where

$$F(x) = \exp(i\Psi(x)), \qquad \Psi(x) = \Phi(x) + iM(x) \tag{71}$$

is one-dimensional disturbance of the wave field produced by object.

It is convenient to rewrite the Eq.(70) in another form containing only one multiplier depending on x before the object function. By simple calculation one has to verify the relation

$$P(x_d - x, z_{do}) S(x - x_s, z_{os}) = S(x_d - x_s, z_{ds}) G(x, x_{ds}, z_{do}, z_{os}) \tag{72}$$

where

$$G(x, x_{ds}, z_{do}, z_{os}) = \left(\frac{z_{ds}}{i\lambda z_{do} z_{os}}\right)^{1/2} \exp\left(-\frac{iK}{2z_{do}}\left[2xx_{ds} - \frac{z_{ds}}{z_{os}}x^2 - \frac{z_{os}}{z_{ds}}x_{ds}^2\right]\right) \tag{73}$$

and

$$x_{ds} = x_d + x_s \frac{z_{do}}{z_{os}} \tag{74}$$

This relation allows us to write the relative disturbance of the wave field from the object as follows

$$\frac{E(x_d, y_d, z_d)}{E_0(x_d - x_s, y_d - y_s, z_{ds})} = \int dx\, G(x, x_{ds}, , z_{do}, z_{os}) F(x) \tag{75}$$

The expression for the relative wave field is convenient despite of the fact that it is not a simple convolution because the propagator G depends only on one variable x_{ds} instead of two variables x_d and x_s. This means that in a small angle approximation each point of the source produces the same image of the object which only becomes shifted on the definite distance. According to the Eq.(74) the shift of point on the source from the origin on the distance x_s leads to a shift of the diffraction pattern as a whole on the distance $-x_s z_{do}/z_{os}$. Thus, there is no necessity to calculate the total diffraction pattern for each point of source because each point produces the same diffraction pattern being only shifted. Therefore we may calculate the interference fringes only for the middle point of the source and afterwards we need to average the resulting intensity over the area having a width $w_s' = w_s z_{do}/z_{os}$ where w_s is the source size (see Fig.16). It is obvious that the fringes with the distance between them p_f less than w_s' will disappear or become much less visible. On the other hand, the fringes with the distance $p_f \gg w_s'$ will be practically undisturbed by the source size. It is easy to understand that the same situation takes place for y coordinate when the object is inhomogeneous in y-direction.

Such a simple analysis allows us to formulate the main recipe for increasing the spatial coherence of in-line experimental scheme. Together with decreasing the source size it is necessary to increase the distance source-to-object compared to the distance object-to-detector. It is of interest to estimate the characteristics of the ESRF (European Synchrotron Radiation Facility) beam lines. The source size of the undulator $w_s \approx 30$ μm, the source-to-object distance $z_{os} \approx 40$ m. With these parameters we calculate that for the object-to-detector distance $z_{do} = 1$ m, the fringes having the distance $p_f > 1$ μm between them can be distinguished.

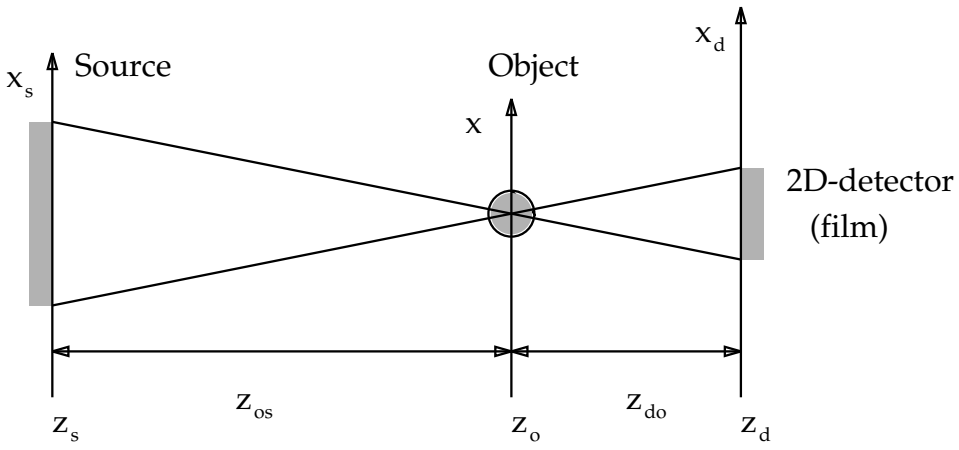

FIG. 16. The finite source size influences the interference pattern by its projection through the object to detector plane

8.2 The conditions of image formation

Keeping in mind the recipe how to take into account the source size we shall consider below the point source at $x_s = 0$. The position sensitive detector can measure the intensity of radiation at each point x_d therefore we are interested in the value

$$I(x_d) = \left| \int dx\, G(x, x_d, , z_{do}, z_{os}) F(x) \right|^2 \tag{76}$$

This value is dimensionless and it describes the intensity of the image normalized on the intensity of spherical wave at the total distance source-to-object z_{ds}. expression. To simplify the problem for the sake of better understanding the characteristic features of the in-line imaging let us assume that the distance source-to-object z_{os} so much larger than the distance object-to-detector z_{do} that we can use the approximation $z_{os}/z_{ds} \approx z_{ds}/z_{os} \approx 1$. In this case only one distance object-to-detector z_{do} is essential in Eq.(76) therefore we may omit the subscript and use z notation for this value. Bearing in mind that we need the intensity we may also omit in the propagator the phase factor which cannot change the intensity. The expression we need now takes the form

$$I(x_d) = |F_i(x_d)|^2, \qquad F_i(x_d) = \int dx\, P(x_d - x, z) F(x) \tag{77}$$

where $P(x, z)$ is the propagator which is defined by Eq.(68) while the function $F_i(x_d)$ can be called image amplitude for the object function $F(z)$.

To understand how the distance object-to-detector z is able to make visible the phase shift let us examine the results of computer calculation of the Eq.(77) for the real model object: round boron fiber of radius $r = 10\,\mu$m and 15 keV energy of X-rays ($\lambda = 0.83$Å),

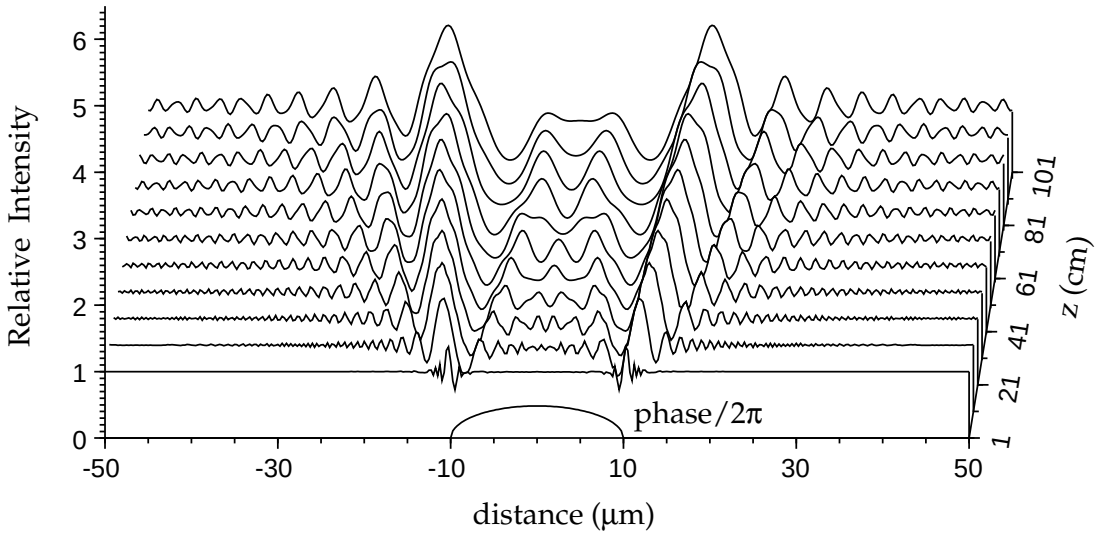

FIG. 17. Holograms of Boron fiber of 10 μm radius with 15 keV energy of X-rays at different distances from the object. On the same axes the phase shift produced by fiber is shown.

shown in Fig.17. The object is very small and absorption equals practically zero. The phase shift is also not large, the maximum value is only π. At short distance $z = 1$ cm the boundaries of the fiber are shown only on the image. At longer distance $z = 21$ cm the additional small oscillations appear while the boundary disturbance of intensity distribution becomes rather significant giving a contrast about 100 per cent. At longer distance the pattern in outside parts of the fiber shadow approximately repeats the pattern of shorter distance but becomes wider (the positions of maximums and minimums are proportional approximately to $\sqrt{z}$). The region of fiber shadow shows the contrast which depends on z in another way and it is approximately similar to the image produced by the slit of different sizes.

The evaluation of the interference patterns at different distances allows us to select three regions:

(1) near field condition (outline imaging) where $\lambda z << r^2$;

(2) intermediate region (Fresnel diffraction) $\lambda z \approx r^2$;

(3) far field condition (Fraunhofer diffraction) $\lambda z >> r^2$.

It is known from the usual optics that the radius of area in transverse plane inside which the phase of spherical wave of wavelength λ at the distance z is less than π equals $\sqrt{\lambda z}$. It is just the radius of first Fresnel zone. Therefore we may formulate these three regions in terms of comparison the radius of object with the radius of Fresnel zone. Under the near field conditions the object covers many Fresnel zones, in case of Fresnel diffraction - only few Fresnel zones, in the case of Fraunhofer diffraction the size of the object is much less than the first Fresnel zone.

Now let us derive these conditions directly from the Eq.(77). First of all, let us verify that the propagator is the normalized function independently on the value of z.

$$\int dx\, P(x,z) = \frac{1}{\sqrt{i\lambda z}} \int dx \exp\left(i\pi \frac{x^2}{\lambda z}\right) = 1. \tag{78}$$

This integral is a particular case of more general table integral

$$\int_{-\infty}^{\infty} dx \exp(-i\beta x + i\gamma x^2) = \left(\frac{i\pi}{\gamma}\right)^{1/2} \exp\left(-i\frac{\beta^2}{4\gamma}\right) \tag{79}$$

where β and γ are arbitrary complex values. I like to call this integral the main tool of the theoretical optics because a lot of problems can be solved using this integral.

Let us consider for the sake of simplicity the pure transparent object. Adding and subtracting the unity to $F(x)$ and using the normalization condition Eq.(78) the expression for the image amplitude can be written as

$$F_i(x_d) = 1 + \frac{1}{\sqrt{i\lambda z}} \exp\left(i\pi \frac{x_d^2}{\lambda z}\right) \int_{-r}^{r} dx\, \exp\left(-i\pi \left[\frac{2x_d x}{\lambda z} - \frac{x^2}{\lambda z}\right]\right) [F(x) - 1] \tag{80}$$

where the integral in the second term is carried out only inside the region where the object changes the phase of wave field and the propagator is written in explicit form.

The first question which arises in the problem of phase contrast imaging is about a sensitivity of the technique. If we analyze a very small object or very slightly scattering

object which produces the small phase shift $\varphi(x)$ we can expand the exponential in the Taylor series after that the image amplitude takes the form

$$F_i(x_d) \approx 1 + \frac{1}{2} a(x_d)\varphi_0, \quad I(x_d) \approx 1 + \varphi_0 \,\mathrm{Re}\, a(x_d) \tag{81}$$

where

$$a(x_d) = \frac{2}{\sqrt{i\lambda z}} \exp\left(i\pi \frac{x_d^2}{\lambda z}\right) \int_{-r}^{r} dx \, \exp\left(-i\pi \left[\frac{2x_d x}{\lambda z} - \frac{x^2}{\lambda z}\right]\right) \frac{\varphi(x)}{\varphi_0} \tag{82}$$

and φ_0 is the maximum phase shift. The maximum contrast $C = \alpha\varphi_0$ where α is a maximum value of the real part of the integral $a(x_d)$ which is close to unity for the parameters of interest (it follows from the computer calculations). On the other hand, the phase $\varphi_0 = 2\pi\delta d/\lambda$ where δ is the decrement of refractive index which has well known dependence on λ as $\delta = \gamma\lambda^2$ and d is the diameter of the object (fiber).

Taking all this into account we obtain a simple formula for the contrast

$$C = 2\pi\alpha\gamma d\lambda \tag{83}$$

which shows the approximate dependence on the wavelength of the radiation. For example, for X-rays of $E = 10$ keV ($\lambda = 1.24$ Å) and for carbon based fiber 0.1 μm thickness the contrast of 2% may be obtained that is experimentally detectable. This estimation was obtained in the paper

- A. Snigirev, I. Snigireva, V. Kohn, S. Kuznetsov and I.Schelokov,
  . Rev. Sci. Instrum. 1995, vol. 66, p. 5486.

where the first experimental results were demonstrated on the phase contrast microimaging.

For larger objects the character of the image depends significantly on the additional term in the phase of propagator $\pi x^2/\lambda z$. Just this term allows to select three regions pointed above. When this part of the phase is small inside the total region of integration, we can neglect it. Afterwards the contrast image amplitude $F_i(x_d) - 1$ becomes the Fourier image of the contrast object function $F(x) - 1$ multiplied by the exponential $\exp(i\pi x_d^2/\lambda z)$, namely,

$$F_i(x_d) = 1 + \exp\left(i\pi \frac{x_d^2}{\lambda z}\right) f_i(x_d), \qquad I(x_d) = |F_i(x_d)|^2 \tag{84}$$

where

$$f_i(x_d) = \frac{1}{\sqrt{i\lambda z}} \int_{-r}^{r} dx \, \exp\left(-\frac{2\pi i}{\lambda z} x_d x\right) [F(x) - 1] \tag{85}$$

It is the case of Fraunhofer diffraction. In the outside parts of the object $x_d >> r$ the Fourier image $f_i(x_d)$ is a slow function and the main features of contrast are defined by just the exponential. This fact explains the law $\sqrt{z}$ in the positions of maximums.

On the other hand, when this part of the phase changes rapidly the integral can be estimated by the stationary phase technique. The Method of Stationary Phase (MSP) is a very powerful technique in theoretical optics. It is a foundation of the geometrical

optics which allows to obtain a solution of many optical problems by simple consideration of ray trajectories. This method in a pure sense allows to estimate approximately the integral

$$Q(q) = \int dx \, \exp\left(i\varphi(q,x)\right) \tag{86}$$

where the phase $\varphi(q,x)$ are slow function of the variable x but it takes very large values. In this case the integrand is strongly oscillating function, therefore the contribution of all regions of integration is very small except only the regions where the phase $\varphi(q,x)$ has zero first derivative. Let us assume, for the sake of simplicity, that we have only one such a point $x_0(q)$ which is a solution of the equation

$$\frac{d\varphi(q,x)}{dx} = 0 \tag{87}$$

This point is just the point of stationary phase. Near this point we may expand the phase as the Taylor series

$$\varphi(x) \approx \varphi(x_0) + \frac{1}{2}\left(\frac{d^2\varphi}{dx^2}\right)_{x=x_0} (x-x_0)^2 + \cdots \tag{88}$$

Now taking into account that only small region near x_0 contributes to the integral we can consider the integral with approximate expression of the phase Eq.(88). However, since other regions don't contribute to the integral we may conserve infinite limits. Then the integral can be calculated analytically using once again the Eq.(79).

$$\int dx \, \exp\left(i\varphi(q,x)\right) \approx (2\pi i)^{1/2} \left(\frac{d^2\varphi(x_0)}{dx^2}\right)^{-1/2} \exp[i\varphi(x_0)], \quad x_0 = x_0(q). \tag{89}$$

Let us consider once again the region $x_d >> r$. In this case the integral without phase shift in the approximation of MSP gives zero contribution while the object of homogeneous structure and approximately round shape, like a fiber, gives only one contribution from one stationary phase point x_0 which is defined from the transcendental equation

$$x_0 = x_d - \frac{\lambda z}{2\pi}\frac{d\Phi(x_0)}{dx}, \qquad F(x_0) = \exp\left(i\Phi(x_0)\right) \tag{90}$$

As a result we obtain

$$F_i(x_d) = 1 + \left[1 + \frac{\lambda z}{2\pi}\frac{d^2\Phi(x_0)}{dx^2}\right]^{-1} \exp\left(\frac{i\pi}{\lambda z}(x_d - x_0)^2\right) F(x_0) \tag{91}$$

The obtained formulas just described the image formation under the near field condition. However, it is not clear directly.

To make clear what physical picture is described by these formulas let us consider the particular case of round fiber once again. In this case

$$\Phi(x) = -\frac{4\pi}{\lambda}\delta\sqrt{r^2 - x^2} \tag{92}$$

where δ is the decrement of refractive index (positive) and expression is valid only for $x < r$. The equation for the stationary phase point now looks as

$$x_0 = x_d - \frac{2z\delta x_0}{\sqrt{r^2 - x_0^2}}$$

When $x_d > r$ and $z\delta$ is small value compared to r, the root of this equation is close to r so we may write $x_0 = r - \varepsilon$ where ε is a small value which can be evaluated in the linear approximation. As a result

$$x_0 = r\left(1 - 2\left(\frac{z\delta}{x_d - r}\right)^2\right) \approx r, \quad \frac{\lambda z}{2\pi}\frac{d^2\Phi(x_0)}{dx^2} = \frac{(x_d - r)^3}{4r(z\delta)^2} \tag{93}$$

Therefore even for small enough radius of fiber we obtain the image amplitude as

$$F_i(x_d) \approx 1 + \frac{4r(z\delta)^2}{[4r(z\delta)^2 + (x_d - r)^3]} \exp\left(\frac{i\pi}{\lambda z}(x_d - r)^2\right) \tag{94}$$

which shows the contrast. The contrast is the larger the smaller the distance from the edge of the fiber $(x_d - r)$. Therefore it is just the outline imaging under the near field condition. For example, the relative region with a contrast larger than 10 per cent may be estimated as

$$b = \frac{(x_d - r)}{r} < 4.5\left(\frac{z\delta}{r}\right)^{2/3} \tag{95}$$

For example, for $z = 1$ cm, $r = 10\,\mu$m, $\delta = 10^{-6}$ we obtain $b = 0.04$.

The expression (94) of the image amplitude has a clear physical sense from the view of geometrical optics. Moreover, it can be accurately obtained in the same form using the geometrical optics approach. Since we consider the relative amplitude the first term corresponds to the ray which go directly from the point source to the point of image x_d. The second term corresponds to the ray which go near the edge of fiber. This ray undergoes the refraction on the boundary of fiber two times: first when it comes in the fiber, second when it go out of the fiber. As a result of refraction the direction of the ray becomes inclined and the ray come in the same point of image x_d being previously at the position of the edge of fiber r (see Fig.2(right)). Therefore the phase shift along the additional path of second ray compared to the path of first ray can be easily calculated. As for the relative amplitude of the second ray we need to consider the density of rays with approximately the same points of arrival x_d. It is not simple even in the geometrical optics. The method of stationary phase allows to make this calculation analytically giving the same result. The intermediate case of Fresnel diffraction is most difficult for the analytical analysis. However, since it is between the clear physically limiting cases it is naturally to expect the intermediate behaviour of the image. It is seen from the computer calculation presented in the Fig.17.

As it is known, the in-line optical scheme is used in the laser optics (coherent) not only for an imaging of objects but also for a registration of holograms which then can be used for a reconstruction of initial wave field at the object and showing the 3-dimensional

image of the object. Because the X-rays are not visible we are interested only in the task of initial wave field reconstruction including the phase shift $\Phi(x)$ from the intensity of the image. Being realized this possibility allows to begin a new branch of tomography of transparent object based of the refraction effect - refraction tomography. Therefore it is of interest to analyze the possible approaches to the solution of this problem. First of all, this task is solved directly in the case of interferometric imaging. Below we consider the possibilities of in-line imaging for a recovering the phase shift. We begin from the standard laser optics scheme.

9. THE PROBLEM OF THE PHASE RETRIEVAL FROM INTENSITY MEASUREMENT IN IN-LINE HOLOGRAPHIC SCHEME

As it is known the procedure of recording the holograms supposes the existence of well known reference beam and interference of this reference beam with the beam scattered by the object. In the in-line scheme such a situation arises only partially in the regions of image plane outside of the image shadow. When object has small size and far field conditions are realized the region of object shadow is small compared to the total region of the object image. This was just the idea of Gabor to use the in-line scheme for recording of the holograms. Below we first consider this case.

9.1 Standard object reconstruction algorithms for far-field conditions

Let us consider once again the Eq.(77) in slightly different notation

$$F_h(x_d) = \int dx\, P(x_d - x, z) F_o(x) = P_z(x_d - x) * F_o(x), \quad H(x_d) = |F_h(x_d)|^2 \tag{96}$$

where $F_o(x)$ is the complex function which describes the wave field disturbance produced by the object, $F_h(x_d)$ is the complex function which describes the wave field disturbance at the distance z from the object. The detector measures the intensity distribution of this field which we shall call the hologram $H(x_d)$. The amplitude $F_h(x_d)$ is connected with the amplitude $F_o(x)$ through the convolution with the propagator function $P_z(x_d - x)$. To shorten the notation we shall use the sign $*$ for the convolution.

The propagator is defined by the Eq.(68). The Fourier image of the propagator is well known. It can be calculated using the main optical tool - the Eq.(79) and equals

$$p_z(q) = \int dx\, \exp(-iqx) P_z(x) = \exp(-i\frac{\lambda z}{4\pi} q^2) \tag{97}$$

Now taking into account the property of the Fourier transformation that the Fourier image of the convolution of two functions equals the product of Fourier images of multipliers and that the exponential contains the distance z in the numerator, it is easy to understand the following properties of the propagator:

$$\begin{aligned} P_{z_1}(x_1 - x) * P_{z_2}(x - x_2) &= P_{z_1+z_2}(x_1 - x_2) \\ P_{z_1}(x_1 - x) * P^*_{z_2}(x - x_2) &= P_{z_1-z_2}(x_1 - x_2) \\ P_{z_1}(x_1 - x) * 1(x) &= 1(x_1) \\ P_0(x_1 - x) &= \delta(x_1 - x) \end{aligned} \tag{98}$$

Here the first relation was used above (see Eq.(69)), the third relation is the statement that the propagator is a nozmalized function (see Eq.(69)), the notation $1(x)$ means the constant function relative to the variable x. The last relation reads that the propagator at zero distance has the property of the Dirac delta-function $\delta(x)$.

Using the properties of the propagator pointed above we may represent the hologram $H(x_d)$ in terms of the contrast function at the object $c_o(x) = F_o(x) - 1$ as follows

$$H(x_d) = 1 + P_z(x_d - x) * c_o(x) + P_z^*(x_d - x) * c_o^*(x) + |P_z(x_d - x) * c_o(x)|^2 \qquad (99)$$

The optical reconstruction technique proposes to illuminate the recorded hologram by the same reference beam and to search the image of the object at the same distance which was used for recording the hologram. However if the object is transparent we cannot find it by looking. The computer allows to reproduce the real experimental situation and it can find the phase shift of the transparent object. Therefore the computed holography reconstruction algorithm considered in different optical papers of last decade

- L. Onural, P. D. Scott, Optic. Engeen. 1987, vol. 26., p. 1124.
- K. A. Nugent, Opt. Commun., 1990, vol. 78, p. 1124
- G. Koren, F. Polack, D. Joyeux, J. Opt. Soc. Amer., 1993,

deals with the integral of back projection of the hologram contrast

$$R_0(x) = P_z^*(x - x_d) * [H(x_p) - 1] \qquad (100)$$

Substituting the expression (99) for the hologram and using the properties of the propagator (98) we arrive to the formula

$$R_0(x) = c_o(x) + P_{2z}^*(x - x_1)c_o^*(x_1) + P_z^*(x - x_d) * |P_z(x_d - x_1) * c_o(x_1)|^2 \qquad (101)$$

What we obtain?. The function contains three terms which are called the object function (in our notation the contrast of object), a twin-image and an intermodulation term. Under the far field condition (Fraunhofer diffraction) when $\lambda z >> r^2$ where now r is the characteristic size of the object, the size of the image is much larger r and the first term just corresponds to focusing the wave field in the small spot of object image (focused object image). The second term corresponds to the wave field of object image at twice distance, therefore it is defocused twin-image, while the third term has a property of smoothed and small in value distribution which looks like a background of the all picture. Such properties of different terms allow us to extract the object image with a good accuracy.

However, even under the far-field condition the function $R_0(x)$ is not an object function in the integral sense because a pure transparent object leads to the relation

$$\int dx R_0(x) = 1(x) * P_z^*(x - x_d) * [H(x_p) - 1] = \int dx_p [H(x_p) - 1] = 0 \qquad (102)$$

The last integral in the Eq.(102) shows simply that the transparent object cannot change the integral intensity. Such a relation is absent for the contrast of the real object function. Therefore the standard reconstruction technique is based on the focusing of the wave field to the object with simultaneous defocusing of all other parts of the image. When the far-field condition is not met the Eq.(101) can be used for the numerical iterative process

when the all terms are taken into account but the first term is used only on the first iteration. However, under the near-field condition when the distance z is small all three term become focused because the propagator $P_z(x_1 - x) \approx \delta(x_1 - x)$ In this case the integral equation 101 is unacceptable completely for a computer calculations.

Among the other numerical algorithms one may consider the Gerchberg-Saxton algorithm which was proposed for the first time for a task of phase retrieval from Fourier transformations in

- R. W. Gerchberg, W. O. Saxton, Optik, 1972, vol. 35, p. 237.

The modified algorithm considers back and forward propagations of any wave field from the hologram to the object and from the object to the hologram. This is one of the different solutions of the standard task of the phase retrieval of complex wavefield from two intensity measurement. We have the relations

$$\begin{aligned} c_o(x) &= P_z^*(x - x_d) * c_h(x_d), \qquad c_o(x) = F_o(x) - 1, \\ c_h(x_d) &= P_z(x_d - x) * c_o(x), \qquad c_h(x_d) = F_h(x_d) - 1. \end{aligned} \tag{103}$$

and we know the intensities $H(x_d) = |F_h(x_d)|^2$ and for the transparent object, for example, $|F_o(x)|^2 = 1$. If the object absorbs the radiation the intensity just after the object also can be measured. Starting with arbitrary phase profile (for example, zero) for $F_h(x_d)$ with known modulus, we obtain $F_o(x)$ with wrong modulus. We replace the modulus by unity and keep the phase and calculate the function $F_h(x_d)$ once again, replace the modulus and so on.

This may be verified directly that under far-field condition this process quickly converges to the solution. The properties of this process in general case can be studied only by computer experiments because the analytical theory is absent. The practice shows that this process converges successfully also in the case when the object covers a limited number of Fresnel zone (Fresnel diffraction) and the outer part of the image recorded is comparable in size with the object shadow. Under the near-field condition this algorithm does not work.

9.2 The problem of the phase retrieval under the near-field condition

As it was shown above, under the near-field condition the image of the transparent object is very different from the real object (see Fig.17). The interference fringes with a small distance between them are localized near the object boundaries while the other part of the object stay practically invisible. It is very difficult to resolve the interference fringes because any detector has a finite spatial resolution. On the other hand, the intensity change in the internal parts of the image is so small that it is difficult to resolve them due to finite sensitivity of the detector. Nevertheless, in recent years several approaches were elaborated for the solution of this problem. The analysis of these approaches leads to the conclusion that these are different only in details while the physical nature is the same. Nevertheless different approaches involve different mathematics and it is necessary to analyze them separately.

Let us consider first the approach which is based on the convolution (96)

$$F_h(x_d) = \int dx\, P(x_d - x, z) F_o(x) \tag{104}$$

and the property of the propagator. This approach was developed in the paper

- V. G. Kohn, Phys. Scripta, 1997, vol. 56, p. 14

The main idea is the following. Since the propagator under the near-field condition is a significantly local function the image of the object at each point is defined by the region of the object projection which is close to this point, and if the rays are only slightly deviated by the object then the change of density of the rays just may be measured in the intensity. The knowledge of the change of rays density allows to recover the angle of their deviation, and the knowledge of the angle allows to recover the phase itself.

The mathematical implementation of this idea looks as follows. We represent the object function as exponential and use the Taylor expansion of the argument near the point of image

$$F_o(x) = \exp\left[\xi(x)\right], \qquad \xi(x) \approx \xi(x_d) + \xi'(x_d)(x - x_d) + \frac{1}{2}\xi''(x_d)(x - x_d)^2 \tag{105}$$

where the argument in general is a complex function

$$\xi = \alpha + i\phi, \qquad \xi' = \frac{d\xi}{dx}, \qquad \xi'' = \frac{d^2\xi}{dx^2} \tag{106}$$

Substituting this approximation to the integral, using the explicit form of the propagator and making the replacement of the variable $x - x_d = x' \to x$ we obtain instead of Eq.(104) the integral in the form

$$F_h(x_d) \approx \frac{1}{\sqrt{i\lambda z}} \int dx\, \exp\left(\xi(x_d) + \xi'(x_d)x + \frac{1}{2}[\xi''(x_d) + i\frac{2\pi}{\lambda z}]x^2\right) \tag{107}$$

Despite the fact that the integrand is a strongly oscillating function we have no problem here because the integral is calculated analytically using the main optical tool - Eq.(79)

$$F_h(x_d) = \exp[\eta(x)] \approx \left(1 - i\frac{\lambda z}{2\pi}\xi''(x_d)\right)^{-1/2} \exp\left(\xi(x_d) + i\frac{\lambda z}{4\pi}\frac{[\xi'(x_d)]^2}{[1 - i\frac{\lambda z}{2\pi}\xi''(x_d)]}\right) \tag{108}$$

To proceed the calculation further we need to assume that the object satisfy the next condition

$$\varphi_0 = \mathrm{Re}\,\frac{\lambda z}{2\pi i}\xi''(x_d) = \frac{\lambda z}{2\pi}\phi''(x_d) << 1 \tag{109}$$

where φ_0 has a sense of the phase which arises in object inside the first Fresnel zone due to only second derivative of the real phase. Under this assumption we may use the Taylor expansion up to second degree. As a result, we obtain the approximate local relation between the logarithms of the object and image functions as follows

$$\eta = \xi + i\frac{\lambda z}{4\pi}\xi'' + i\frac{\lambda z}{4\pi}[\xi']^2\left(1 + i\frac{\lambda z}{2\pi}\xi''\right) - (\frac{\lambda z}{4\pi})^2[\xi'']^2 = \beta + i\psi \tag{110}$$

We are interested in the real part of this relation which is connected with the image intensity. This equation represents by itself the differential equation for the phase of the object function. It is convenient to write this equation in terms of variable

$$x_0(x) = \frac{\lambda z}{2\pi}\frac{d\phi(x)}{dx} \tag{111}$$

and in the form which is convenient for the iterations

$$x_0' = \frac{2(\alpha-\beta) - \varepsilon^2(\alpha'^2\alpha'' + \frac{1}{2}\alpha''^2) - 2\alpha' x_0 + \alpha'' x_0^2 + \frac{1}{2}x_0'^2}{1 - 2\alpha' x_0}, \quad \varepsilon = \frac{\lambda z}{2\pi}. \tag{112}$$

This is the main equation of the algorithm of the phase retrieval. It is convenient for the iterations because does not contain the fast oscillating exponential.

At the first step of calculation one deals with the equation

$$x_0' = 2(\alpha - \beta)$$

which in usual notation looks as follows

$$\frac{d^2\phi(x)}{dx^2} = -\frac{K}{z}\ln\left(\frac{H(x)}{I(x)}\right) = -\frac{K}{z}\ln\left(1 + \frac{H(x) - I(x)}{I(x)}\right) \approx -\frac{K}{I(x,z)}\frac{dI(x,z)}{dz} \tag{113}$$

where $I(x) = |F_o(x)|^2$. The last approximate relation allows us to understand the connection with other approaches.

Thus, the Eq.(112) in a good tool for making the calculation on the phase retrieval. However, this equation is valid only under the assumption (109) which means that we may retrieve the phase only in the "area image" case. In the "boundary image" regions it is not working. The main reason of this fact is that the approach suppose that number of rays in each part of image is the same at an object and only the density of rays (the distance between them) can change due to the refraction. However, the degree of ray inclination at the boundary and in internal part of image may differ significantly for thick enough objects of approximately round form. If the distance z is so small that this condition satisfies for all image that internal part will practically invisible and only very narrow region near the boundary will be seen. In addition the distance turns out to be very small. In a real situation with imaging the object like the fiber the condition (109) is not met. The rays intersect each other and the strong interference takes place which leads to strong oscillations of intensity in the hologram (see Fig.18(left)).

To avoid this complexity in the paper pointed above the proposal is considered to average the real intensity of the hologram over these oscillations. This operation allows to kill the interference between the rays but conserve the middle density of the rays. After that the intensity distribution becomes suitable for a calculation and the phase retrieval. Evidently, the procedure of averaging does not allow to reproduce the sharp boundaries and these are retrieved as smoothed. However, in general the method works successfully as it is shown in the Fig.18(right). As for the objects without the sharp boundaries or when the jump of susceptibily values is not large, the method allows to retrieve them without an averaging.

For the sake of simplicity we consider only the one-dimensional object like a fiber. The two-dimensional objects like a sphere also can be considered. In this case only the mathematics becomes more difficult but the ideas are the same. It was done in paper

- K. A. Nugent, T. E. Gureyev, D. Cookson, D. Paganin, Z. Barnea,
  . Phys. Rev. Lett. 1996, vol. 77, p. 2961.

However it is useful to consider the two-dimensional case from other position - direct Maxwell's equation. In Section 1 when we consider the geometrical optics we neglect the higher derivative of the phase. Now let us go out of the geometrical optics and consider once again the accurate equation (4) for the intensity but in empty space when the susceptibility equals zero

$$\mathrm{grad}\phi(\mathbf{r}) \cdot \mathrm{grad}I(\mathbf{r}) + \mathrm{grad}^2\phi(\mathbf{r}) \cdot I(\mathbf{r}) = 0 \tag{114}$$

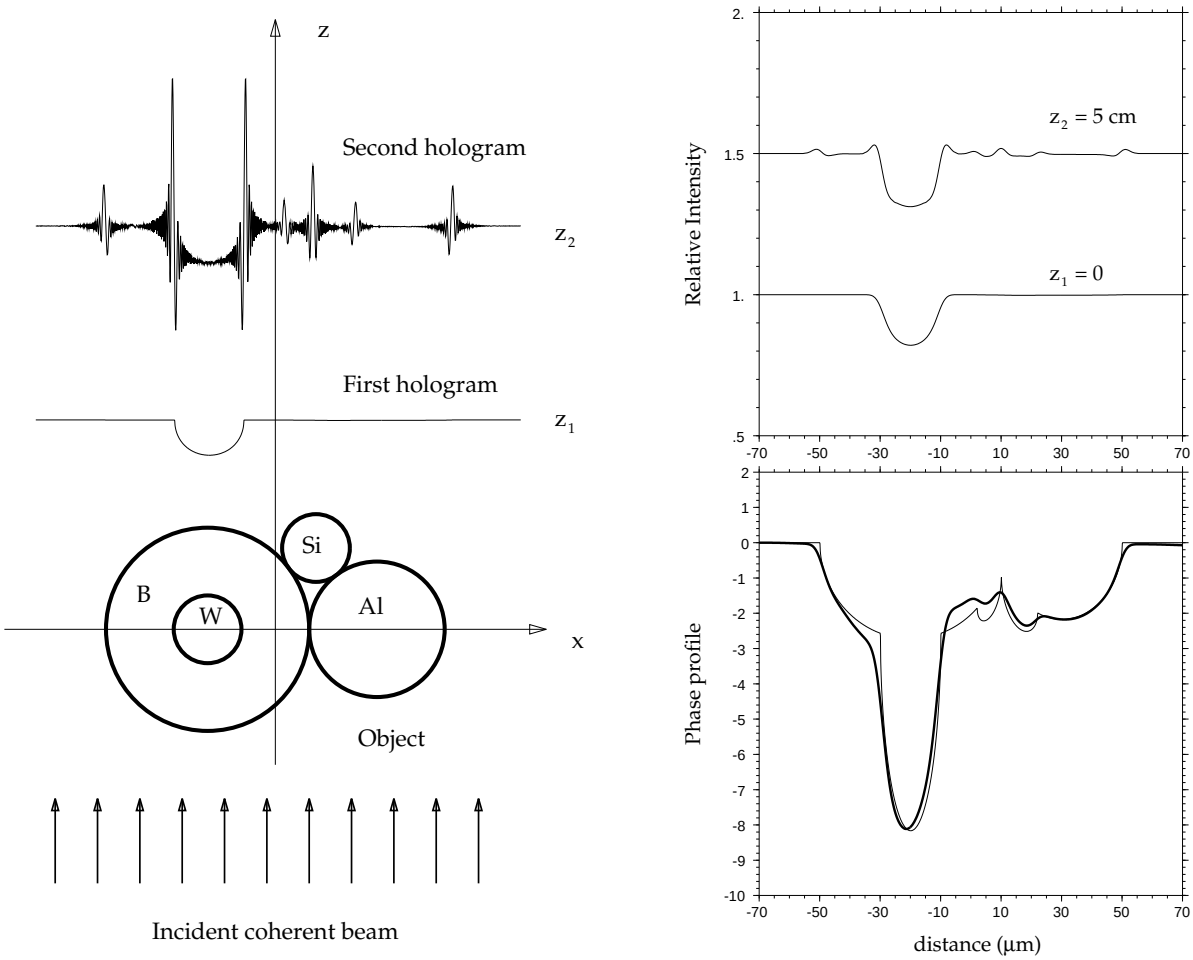

FIG. 18. The model object - a set of fibers: Boron (radius 30 μm), Tungsten (radus 10 μm), Aluminium (radius 20 μm) and Silicon (radius 10 μm) and its holograms at the distances $z_1 = 0$ and $z_2 = 5$ cm (Left); the same holograms smoothed by a Gaussian of 5 μm halfwidth (right, top); The original (thin curve) and reconstructed from the smoothed data (thick curve) phase profiles (right, bottom)

Now let us assume that the phase of the wavefield is described by the formula

$$\phi(\mathbf{r}) = Kz + \varphi(r_\perp) \tag{115}$$

Then from the accurate Eq.(114) we immediately obtain

$$-K\frac{dI(r_\perp, z)}{dz} = \nabla_\perp[I(r_\perp, z)\nabla_\perp\varphi(r_\perp)] \tag{116}$$

This equation is accurate if the Eq.(115) is accurate. However, the Eq.(115) can be accurate only with $\nabla_\perp\varphi = 0$ because $(\nabla\phi)^2 = K^2$. Nevertheless even when $\nabla_\perp\varphi \neq 0$ this equation may be used for the analysis of the transport of intensity due to inhomogeneous transverse distribution of the phase. This equation was considered in the paper

- T. E. Gureyev, A. Roberts, K. A. Nugent,
  J. Opt. Soc. Amer., 1995, vol. A12, p. 1932.

for a phase retrieval problem when, on the other hand, was proposed to determine the phase distribution of the wave field from known intensity distribution along the optical axis. As usual, it is enough to use two points on the z-axis.

In the particular case when we can neglect the transverse derivatives of intensity compared to the same for the phase (it is really so for the transparent object and near-field condition without the ray interference) then the equation may be rewritten in the form

$$-K\frac{dI(r_\perp, z)}{dz} = I(r_\perp, z)\nabla_\perp^2\varphi(r_\perp) \tag{117}$$

This equation is a two-dimensional equation. In the one-dimensional case it coincides with the Eq.(113). The method using the two-dimensional propagator allows to write the more complicated equation for iterations where the Eq.(117) will be a start approximation. However even in the frame of start approximation the problem is not simple mathematically.